INTERFACE

rsif.royalsocietypublishing.org

Review

**Cite this article:** Schöne A-C, Roch T, Schulz B, Lendlein A. 2017 Evaluating polymeric biomaterial–environment interfaces by Langmuir monolayer techniques. *J. R. Soc. Interface* **14**: 20161028.
http://dx.doi.org/10.1098/rsif.2016.1028

Received: 19 December 2016
Accepted: 5 April 2017

**Subject Category:**
Reviews

**Subject Areas:**
biomaterials

**Keywords:**
Langmuir monolayer, biodegradable polymers, air–water interface, protein Langmuir layers

**Author for correspondence:**
Andreas Lendlein
e-mail: andreas.lendlein@hzg.de

THE ROYAL SOCIETY
PUBLISHING

# Evaluating polymeric biomaterial–environment interfaces by Langmuir monolayer techniques

Anne-Christin Schöne[1,2], Toralf Roch[2,3], Burkhard Schulz[1,2] and Andreas Lendlein[1,2,3]

[1]Institute of Chemistry, University of Potsdam, Karl-Liebknecht-Strasse 24-25, 14476 Potsdam, Germany
[2]Institute of Biomaterial Science and Berlin-Brandenburg Centre for Regenerative Therapies (BCRT), Helmholtz-Zentrum Geesthacht, Kantstrasse 55, 14513 Teltow, Germany
[3]Helmholtz Virtual Institute-Multifunctional Biomaterials for Medicine, Kantstrasse 55, 14513 Teltow, Germany

AL, 0000-0003-4126-4670

Polymeric biomaterials are of specific relevance in medical and pharmaceutical applications due to their wide range of tailorable properties and functionalities. The knowledge about interactions of biomaterials with their biological environment is of crucial importance for developing highly sophisticated medical devices. To achieve optimal *in vivo* performance, a description at the molecular level is required to gain better understanding about the surface of synthetic materials for tailoring their properties. This is still challenging and requires the comprehensive characterization of morphological structures, polymer chain arrangements and degradation behaviour. The review discusses selected aspects for evaluating polymeric biomaterial–environment interfaces by Langmuir monolayer methods as powerful techniques for studying interfacial properties, such as morphological and degradation processes. The combination of spectroscopic, microscopic and scattering methods with the Langmuir techniques adapted to polymers can substantially improve the understanding of their *in vivo* behaviour.

## 1. Introduction

Biomaterials are used in contact with living tissues or organisms as, for example, in medical devices [1]. Depending on their application, different demands have to be fulfilled concerning the mechanical, physical, chemical or biological functionalities. Polymeric biomaterials are of great importance for medical and pharmaceutical applications as a wide range of properties and functionalities can be achieved by specific tailoring [2–7]. They can be categorized in two groups: naturally occurring and synthetic materials. Alginates, silk and proteins, including collagens, are typical examples of biopolymers derived from natural resources [8]. Typical synthetic polymers in medical applications are aliphatic polyesters, polyanhydrides or polyamides [6,9,10]. Both groups can be further divided into two classes: non-biodegradable and biodegradable polymers. Biodegradable polymers are of special interest because of their applicability for tissue regeneration and drug delivery systems supported by their tailorable mechanical properties, morphological structures [11–13] and degradation behaviour, which are adjustable by the variation of the monomer structure, copolymerization, blending or molecular architecture. The implantation of synthetic materials is orchestrated by a sequence of the body's own (defence) mechanisms that aim to separate the implant from the rest of the body in order to prevent it from doing harm [14]. This physiological response is predominantly mediated by the immune system and should result in the encapsulation of the foreign body. Therefore, the major challenges for the application of biomaterials in medicine are to control foreign body reactions (FBRs) and simultaneously facilitate regenerative processes [15]. Interestingly, FBRs can occur immediately after implantation or be delayed, often by several

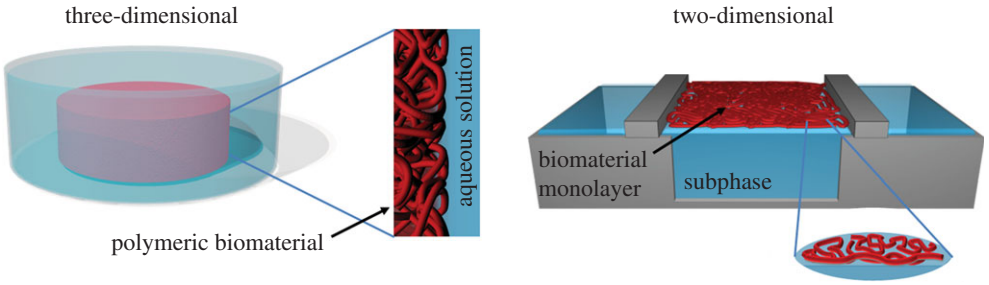


**Figure 1.** Three-dimensional biomaterial–environment interface compared to the two-dimensional layer at the air–water interface.

years, and can have acute or chronic characteristics. The delayed reaction implies that changes occurring on the implant interface, for example, induced by degradation processes can trigger immunological reactions. However, degradation processes, especially enzymatically mediated degradation as occurring *in vivo*, are insufficiently understood. Furthermore, a description at the molecular level is required to gain better understanding of the interactions between biological systems and synthetic materials occurring at the material–bioenvironment interface. Additionally, the material surface topography plays an important role on the cellular response [16] and is a key factor for the differentiation of mesenchymal stem cells *in vitro* [17], for example. The interaction of the bioenvironment with polymer materials is commonly investigated by cell-culture techniques and afterwards characterized using, for instance, direct visualization by microscope [18], providing a wide range of information such as morphological changes, detachment forces, kinetics of cell attachment, aggregate size distribution over the time or intra- and extracellular protein expression. However, the interaction of biomolecules with a biomaterial surface at the molecular level is still challenging and requires the comprehensive characterization of surface properties. Several methods to create (ultra)-thin films are described including the self-assembled monolayer method, [19] layer-by-layer (LBL) technique [20,21], coating [22], printing [23] and Langmuir [24] techniques. The LBL technique has received much attention for the preparation of mono- and multilayers due to the mild preparation conditions from solution and the obtained layers reveal a relatively open structure allowing diffusion of components if required. An efficient and precise method to investigate interfaces is the Langmuir technique where monomolecular films are formed at the air–water interface, which are physical models of interfaces with unique properties [25]. They also enable a fast evaluation of degradation processes and a separation of chain scission kinetics from the transport processes during the degradation. Langmuir monolayers also allow the investigation of interaction between a polymer and its environment with a two-dimensional approximation (figure 1). Different types of experimental techniques to determine interfacial tension are known such as the Wilhelmy plate, the pendant drop and the capillary rise technique [26]. Langmuir layers formed through lateral compression enable the control of the film thickness, whereby their packing density, orientation and conformation can be tailored. To gain a deeper insight into interfacial behaviour of macromolecules, the description of thermodynamic and kinetic processes on the surface as well as the adsorption and ordering processes or degradation behaviour can be analysed. By spreading water-insoluble substances at the air–water interface, a Langmuir layer is formed, whereas by injecting substances able to dissolve into the subphase a Gibbs layer is formed by adsorption. The formation of a Langmuir layer from organic solvent occurs by the arrangement of amphiphilic molecules directly at the air–water interface and is studied as a function of the surface area $A$, whereby Gibbs layers are obtained due to the adsorption of surface-active molecules at the interface and are studied as a function of the surface concentration. The amount of molecules at the interface depends on the equilibrium between adsorption and desorption, which is adjustable, for example, by the pH value, salt concentration, ionic strength, co-components in the subphase and temperature. Both approaches allow the detailed investigation of molecules with biological relevant substances using different physical and chemical analytical techniques.

For example, using the Langmuir method the characteristics of protein layers can be manipulated in a very controlled fashion by tuning the molecular packing and two-dimensional order. Thus, conformation transitions or morphological changes of adsorbed proteins depending on interfacial forces or subphase parameters are investigated [27,28]. A clinically relevant example is the activation of the complement cascade by synthetic surfaces in cardiovascular implants or dialysis devices [29–31]. How exactly the proteins arrange at polymeric biomaterial surfaces and what kind of features lead to conformational changes and partial or complete denaturing of proteins are open questions.

Additionally, regarding the degradation of synthetic polymers not only the degradation behaviour of the material surface has to be considered, but also the bioresponse of the released degradation fragments. Applying Langmuir techniques opens different ways to elucidate these questions. First, the formation of Langmuir or Gibbs layers based on polymers allows the investigation of their interfacial properties and the morphological re-arrangement under compression (figure 2*a*). Additionally, the transfer of such layers onto a solid substrate enables the characterization by diverse techniques and the implementation of cell-culture experiments. Second, the evaluation of interactions between polymer Langmuir layers and subphase components, such as enzymes or degradation fragments, simulates the biomaterial–environment interface *in vivo* (figure 2*b*). Third, the investigation of the degradation behaviour of polymers at the air–water interface avoids any diffusion processes and allows studying the degradation processes at the molecular level.

This review will discuss the potentials of Langmuir monolayer methods to understand polymer monolayers, their degradation behaviour and how they can be used to investigate protein behaviour on implant interfaces. The manuscript focuses predominantly on the preparation and characterization of polymer-based Langmuir layers, while (phospho)lipid layers at the air–water interface, which are

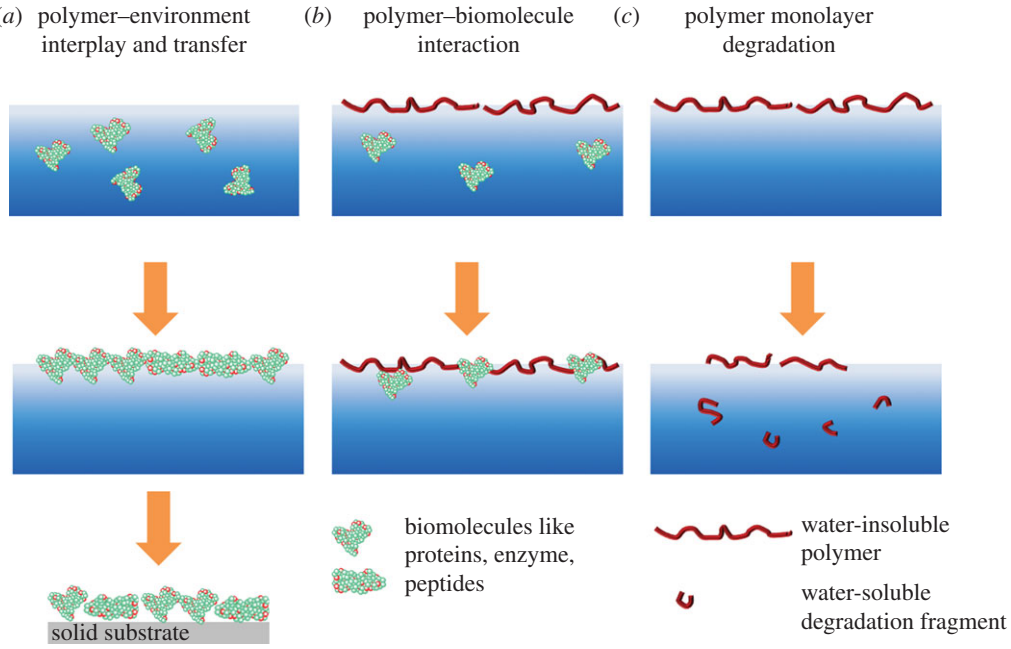


**Figure 2.** (*a*) Well-defined Langmuir monolayers prepared from synthetic or natural (shown) polymers, which can be transferred onto a solid substrate, (*b*) synthetic biomaterial surface interacting with proteins and (*c*) polymer layer during degradation. (Online version in colour.)

frequently discussed as a model system for cell membranes [32–36], are not considered. It is not the aim to completely cover the literature; however, previous reviews and overviews are cited to provide further information on this comprehensive topic. Representative papers have been selected revealing the special interest on protein and polymer orientations at the interface relating to their ability to interact with the environment.

## 2. Langmuir monolayer techniques

### 2.1. General principles

The Langmuir monolayer technique is based on the results of the research from Lord Rayleigh and Agnes Pockels at the end of the nineteenth century [37,38]. Basically, at constant temperature the surface pressure–area ($\pi$-$A$) isotherm is recorded by measuring the surface pressure $\pi$ which is the difference between the surface tension of the pure subphase and the surface tension of the subphase covered by the spread monolayer during reduction or expansion of the covered surface area ($A$). The shape of the $\pi$-$A$ isotherms depend, among other aspects, on the nature of amphiphiles, compression speed, spreading conditions and temperature. For classical amphiphiles, the isotherm can roughly be classified into four different regions and the corresponding transition regions: a two-dimensional gaseous (G) phase, a liquid-expanded (LE) phase, followed by liquid-condensed (LC) and a two-dimensional solid (S) phase, where the maximally reached surface pressure is called the collapse pressure (figure 3) [39,40]. Between the G and LE and the LE and LC phases, first-order transition takes place revealing a (pseudo)plateau region (coexisting region). Not all phases occur for every amphiphile and differ depending on the experimental conditions. In particular, the interpretation of polymeric $\pi$-$A$ isotherms is usually more complex because of the macromolecular conformational flexibility and the resulting architecture such as coils, pancakes, crystals and liquid crystals [41–43].

Low molecular weight amphiphiles, including (phospho)lipids and organic surfactants, are used initially for the formation of Langmuir layers due to their appropriate hydrophilic–hydrophobic balance, enabling the molecular orientation at the air–water interface. In the middle of the twentieth century, the idea of Langmuir monolayers was extended towards the description of the film formation of non-classical amphiphilic materials, such as (poly)peptides [44,45], proteins, [46] polysaccharides [47], nanoparticles [48], dyes [49,50], fullerenes [51–53] and (biodegradable) polymers [54,55].

A variety of sensitive methods enable the *in situ* characterization of the monolayers at the air–water interface, including microscopy, spectroscopy and scattering techniques. For example, Brewster angle microscopy (BAM) is used to visualize (in)homogeneities in the optical properties of the film by monitoring domain formation or variations in monolayer thickness and other morphological changes [56,57]. Dielectric properties and thicknesses of the monolayers can be obtained by (spectroscopic) ellipsometry [58,59], whereas the structural and orientational changes in the monolayer can be obtained by infrared reflection-absorption spectroscopy (IRRAS) [60–62]. Two types of spectral information are obtained from IRRAS: frequency and intensity changes. Frequency changes provide information about the molecular structure and interactions, whereas the quantitative evaluation of the measured band intensities allows the determination of the chain and group orientations. Grazing incidence X-ray diffraction provides information only about ordered domains within the monolayer [63,64], whereas specular X-ray reflectivity (XR) supplies access to the electron density distribution across the layer, allowing speculation about the monolayer profile constitution.

The transfer of monolayers from the air–water interface onto a solid substrate after the compression into a highly condensed state allows the preparation of organized mono- and multilayer structures with varying layer compositions and orientation and enables the modification of the biomaterial surface directly. A recent review summarized the LB research

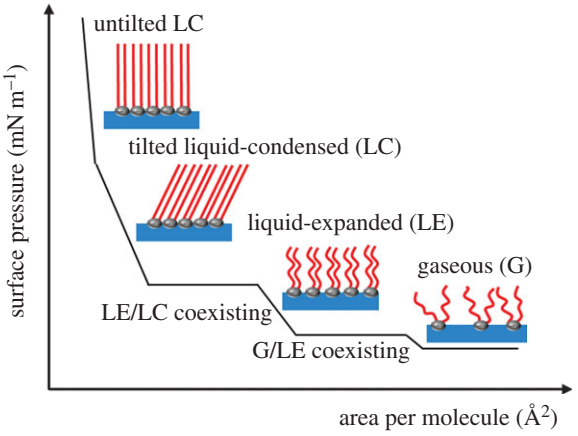


**Figure 3.** Illustration of a surface pressure–area isotherm for low molecular weight surfactants with their possible phase state. (Online version in colour.)

in surface sciences, physical chemistry, materials chemistry and nanotechnology [24]. The LB technique is also used for the elucidation of membrane surfaces, capsulation technologies, surface patterning, and for electronic and optical applications [65].

By vertical dipping of a hydrophilic or hydrophobic solid substrate into the subphase, the film can be transferred. By repeating the transfer process, different deposition types of the multilayers are formed [66]. However, the transfer is not limited to vertical dipping method. In the Langmuir Schaefer (LS) technique, the film is transferred by horizontal dipping through stamping the solid substrate [66–68]. Moreover, the layer can be transferred from the aqueous subphase onto a solid substrate by gradually lowering the water level relative to the substrate. Compressed Langmuir monolayers are not in their thermodynamical equilibrium resulting very often in morphological changes (e.g. crystallization or aggregation) during and after the transfer process. This has to be considered for interpretation of the LB film structures and properties in comparison with the virgin Langmuir films. Almost all surface characterization methods are suitable for the description of the transferred layer, contributing to the knowledge of the monolayer assembly [24,69,70]. Several methods are used to quantify topography, thickness and morphologies, for example atomic force microscopy (AFM) [71–73], scanning electron microscopy [74,75], transmission electron microscopy (TEM) [76,77] or ellipsometry [78]. Additionally, information on interfacial properties and orientation of molecules are provided by infrared [79], UV-vis and fluorescence spectroscopy [80], X-ray techniques [81] and Fourier transform infrared spectroscopy [82].

### 2.2. Polymer-based Langmuir layers

A variety of synthetic and natural polymers having different chemical structures are used to form Langmuir layers at the air–water interface. To emphasize the varieties in the chain orientation of polymeric monolayers, three different polymer systems are exemplarily outlined in figure 4. For each system, small changes in the chemical structure, the composition, molecular weight distribution, hydrophilicity or the tacticity result in different chain orientation and packing motifs.

In 'amphiphilic polymers', each repeating unit has an amphiphilic character given by the ratio of the hydrophilic to hydrophobic parts and forms high ordered structures [86,87]. Polymethacrylates [88] and poly(maleic acid) derivatives are typical polymers in this class. Polymer brushes, where the backbone and the side groups exhibit different hydrophilicity/hydrophobicity, belong to this amphiphilic polymer class. Alternatively, amphiphilic block copolymers composed of a hydrophilic segment, such as polyethylene glycol, and a hydrophobic segment, such as polystyrene, also form stable monolayers [89,90]. Under compression, such block copolymers form brushes at the interface [91]. By contrast, hairy-rod polymers are composed of rigid rod-like back bones surrounded by flexible side chains [92–94]. Cellulose derivatives [92] and glutamates [95], which form stiff α-helices by hydrogen bonding, but also aromatic polyguanamines [96] belong to hairy-rod macromolecules. Unlike hairy-rod and amphiphilic copolymers, the amphiphilic character of polymers such as aliphatic polyesters, polyanhydrides or polycarbonates, which are frequently used in clinical applications, is caused by the presence of hydrophobic parts (aliphatic chains) and hydrophilic binding groups such as ester bounds in the backbone itself. The polar groups of these macromolecules allow their nearly plane arrangement at the interface with a pancake-like structure. Varying the hydrophobic segments between hydrophilic groups in the macromolecular chain influences their spreading behaviour and packing motifs. In the following, we concentrate on those non-classical amphiphilic polymers, namely aliphatic polyesters and proteins.

## 3. Polymers at the air–water interface and on solid substrate

### 3.1. Pressure-induced morphological changes in synthetic polymer layers

Poly(ε-caprolactone) (PCL)-based materials reveal high degradation stability, whereby the degradation velocity can be varied by copolymerization or by the creation of advanced polymer architectures [97–99]. At the air–water interface, PCL forms closed-packed two-dimensional monolayers below the collapse point [100]. Above this point, crystallization from supersaturated solution occurs, which has been traced by *in situ* BAM [85]. By varying the compression speed and molecular weight of the PCL, different sized crystals are formed [85,101,102]. Expansion of the film leads to the detachment of the polymer chains from the crystalline domains, which is typically called 'melt' process, followed by re-formation of a monolayer. Remaining crystallites serve as nucleation centres for the next crystallization process in the second compression run. Modification of the interfacial properties as well as the film morphology of PCL-based Langmuir films has been performed by blending or copolymerization. The interfacial properties of PCL/polystyrene (PS) blends are dominated by the polyester [103], whereas the film morphology is determined by the blend composition, which is in agreement with structures observed in polymer blends of amphiphilic and non-amphiphilic polymers at the air–water interface [104]. Copolymerization prevents the phase separation. For example, the introduction of urethane junction units results in a decreased crystallization tendency and a closer film packing due to the formation of hydrogen bondings [105]. The introduction of polyethylene glycol (PEO) blocks in linear and grafted block copolymers (PCL-*b*-PEO) leads to the formation of a transition region before

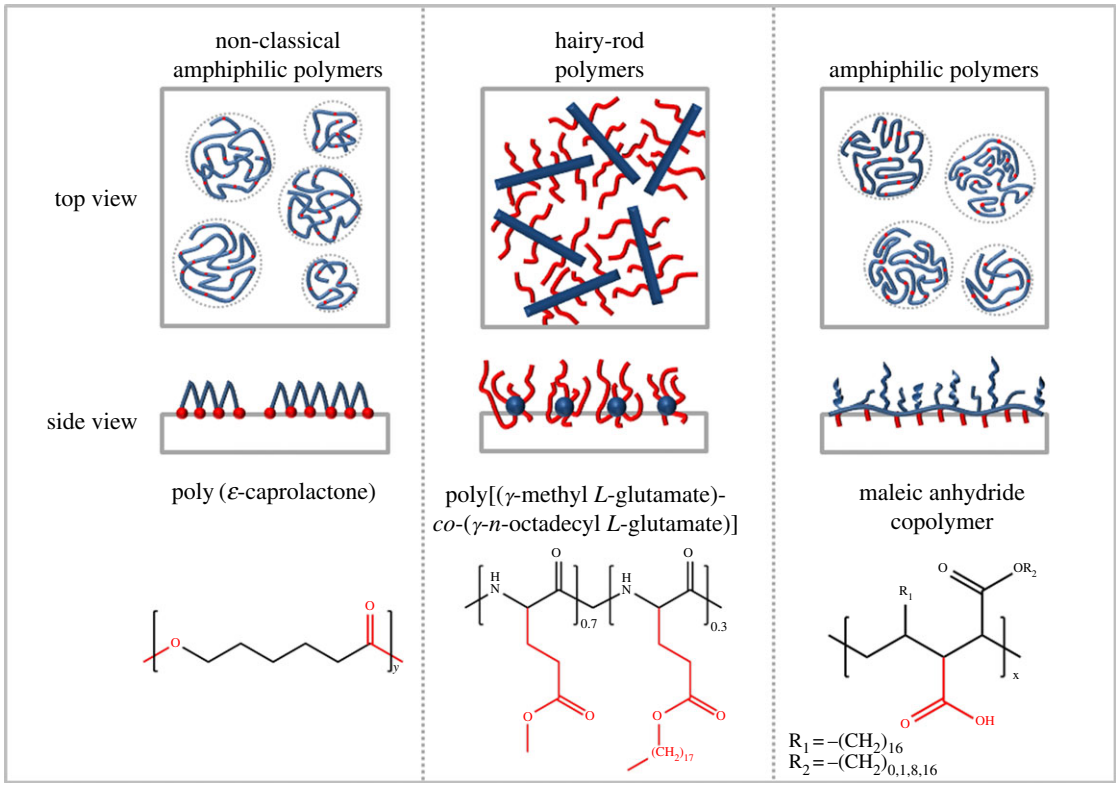


**Figure 4.** The interfacial behaviour of synthetic non-classical amphiphilic polymers, hairy-rod polymers and amphiphilic polymers is shown as top and side view in a medium compressed state. One polymer is given as an example for each group by name and chemical structure [83–85]. (Online version in colour.)

film collapse [106,107]. PEO segments dissolute in the subphase, whereby the PCL segments are still able to crystallize, which is revealed by AFM at transferred LB films. For five-arm star-shaped molecules based on PEO-*b*-PCL block copolymers, the PEO core units impact the PCL crystal shape in transferred LB layers, but not the crystal height (7.5 nm) [106], which is in the same range as for linear PCL crystals at the air–water interface [85]. AFM investigation of grafted copolymers of PCL and poly(glycerol adipate) (PA-*g*-PCL) reveals a film thickness of approximately 7.6 nm by reduced crystal size and lower crystallization rate compared to the homopolymers, which approve the high crystallization tendency of PCL chains at the air–water interface [107]. The introduction of hydrophilic poly(*p*-dioxanone) (PPDO) blocks giving PDC multiblock copolymer leads to an enhanced collapse tendency with increasing PPDO content, which is the result of the increased number of polar groups [108].

Regarding the interfacial properties of poly(lactic acid) (PLA), two different isomers have to be considered, poly(L-lactic acid) (PLLA) and poly(D-lactic acid) (PDLA) [76,109]. The $\pi$-*A* isotherms for PLLA and PDLA monofilms are identical; however, blends of PLLA and PDLA (*rac*-PLA; 50 : 50 wt%) reveal monolayers with different interfacial properties due to a different packing of the chains caused by stereo complexation [110]. This different packing of the chains is confirmed by IRRAS investigations, which show distinctions in the conformation of the helical chains in the compressed monofilms. The compression of poly[(*rac*-lactide)-*co*-glycolide] (PLGA; 50 wt% *rac*-PLA) monolayers reveals a more expanded behaviour with a gradual increase of the surface pressure compared with PLA monolayer [111–113]. For PLA layers, a nucleation process is observed during phase transition, while continuous wormlike structures are visualized in the condensed phase by AFM (figure 5*a*) for PLGAs due to the hydrophobic interactions [112]. *In situ* BAM investigations of PLGA monolayers confirmed circular aggregates at the air–water interface in the transition state. Moreover, these aggregates are able to form a network-like structure under constant surface pressure and surface area conditions (figure 5*b*). The comparison of *in situ* BAM measurements with *ex situ* AFM images evidences that transferred LB layers do not reflect quantitatively the morphology of a water swollen layer at the air–water interface. A retarded percolation of the monolayer compared to PLGA has been observed for oligo[(*rac*-lactide)-*co*-glycolide] (OLGA)-based polyesterurethanes, which are synthesized by the use of urethane junction units as chain extenders [114]. The retarded percolation is caused by a slightly increased stiffness and lower mobility caused by a higher H-bonding capacity, which has, however, no influence on the layer thickness. At the molecular level, the mechanisms responsible for the transient glass transition behaviour have been investigated by X-ray reflectivity and double-wall-ring interfacial rheometry at the air–water interface [115].

## 3.2. Proteins at the air–water interface

Protein-based layers are of high interest for biomedical applications as they interlink the artificial interface and the cellular compartments, including immune cells, stem cells and tissue cells. The majority of the studies investigating protein monolayers used bovine serum albumin (BSA), which is a valid model protein for fundamental studies since it is available in high amounts and well understood, whereas its clinical relevance is rather limited. Recently, in several studies monolayers of other proteins were investigated including extracellular matrix components and immunoglobulins,

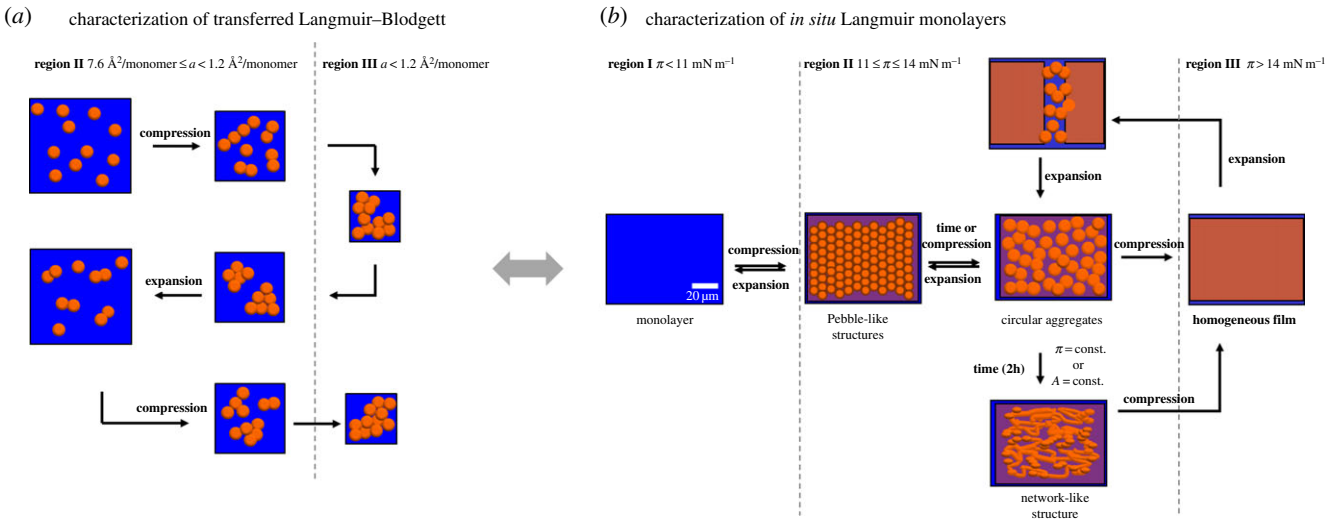


**Figure 5.** Formation of a PLGA network-like structure (*a*) during repeated compression–expansion cycles based on Langmuir and AFM investigations and (*b*) at the air–water interface and its reversibility. The orange circles represent the collapsed domains; the blue and tinted orange background represent the water surface and the flat polymer monolayer area, respectively. (*a*) Adapted with permission from [112]. Copyright 2012 American Chemical Society. (*b*) Reproduced with permission from [114] © 2015 WILEY-VCH Verlag GmbH & Co. KGaA, Weinheim. (Online version in colour.)

indicating an increasing interest and expectation to obtain new insights in protein behaviour, which might also be relevant for specific applications. For the preparation of such protein layers, several approaches have been employed including physical adsorption [116] and site-specific immobilization [117].

The interactions of biomolecules and nanomaterials with classical amphiphilic Langmuir monolayers as a model system for cell membranes were recently reviewed [32]. Therefore, the interactions of proteins with amphiphilic Langmuir layers are not considered here. We discuss a few pure protein-based Langmuir layers as representatives for biomacromolecules.

A wide range of proteins, including albumins, are water-soluble, forming Gibbs layer at the air–water interface. The flexible structures of the molecules allow conformational changes depending on the experimental conditions. Different parameters such as subphase pH value, ionic strength, temperature or spreading solvent affect the film stability at the interface [118]. Transfer of the protein layers by the LB technique requires the selection of the optimal experimental conditions in terms of temperature, surface pressure and solid substrate material. Protein solutions with high concentrations lead to unordered and loosely packed protein layers with granule structure, which could partly be denatured hindering the formation of closely packed or ordered arrays [119]. When using proteins for Langmuir monolayer studies, a few possible obstacles need to be considered. First, recombinant proteins generated by overexpression in bacteria, such as *Escherichia coli*, lack post-translational modifications such as glycosylation. A second aspect to be considered is the purity of proteins, since impurities caused by contaminating proteins or peptides, but also residual bacterial compounds such as endotoxins, could substantially bias the experimental readout.

### 3.2.1. Bovine and human serum albumin

Albumins are applied in clinical chemistry and cell-culture media [120]. Recently, the two-dimensional behaviour of serum albumins was reviewed summarizing the characterization of protein–lipid interactions, protein–ionic surfactant interactions, protein insertion into monolayers and topographical studies [46]. Owing to its stability, BSA is frequently used as an example protein for fundamental studies, but also for the development of immunosensors and for surface passivation [121,122].

Spreading a BSA solution at the air–water interface results in an immediate jump up of the surface pressure reaching a plateau value within approximately 900 s, independent of the subphase (water, buffer, clay mineral: saponite dispersion) [123]. However, the maximum of the attained surface pressure depends on the type of subphase. Adding clay mineral or buffer, the equilibrium surface pressure increases compared to water. The adsorption process of molecules occurs in two steps. Initially, the BSA diffuses from the subphase to the interface, followed by a re-arrangement of the molecules. Afterwards, BSA molecules are able to incorporate in the existing interface layer increasing the surface pressure to positive values until an equilibrium surface pressure is reached. Figure 6 represents several possible arrangements of globular proteins such as BSA at the air–water interface [124]. Adding phosphate buffered saline (PBS) increases the surface charges and leads to a slightly higher surface tension (53 mN $m^{-1}$) and increases the layer thickness, while simultaneously decreasing the refractive index and the surface density.

Variation of the subphase pH leads to a modified time to reach the surface pressure equilibrium [125]. Below the isoelectric point (pH 3.8) BSA is positively charged and in its F form, where most hydrophobic residues are located at the outer shell, leading to a high driving force directed to the interface. Close to the isoelectric point (pH 5.1) BSA is in a compactly packed N form and at pH 8.2 (above the isoelectric point) the BSA molecules are negatively charged and in the B form. The B form is more expanded compared with the N form, exposing the less hydrophobic segments to the subphase. The negative surface pressure values after spreading indicate directly that the rearrangement of BSA leads to a reduction of projected surface area per molecule. Surface dilational elasticity measurements do not indicate significant

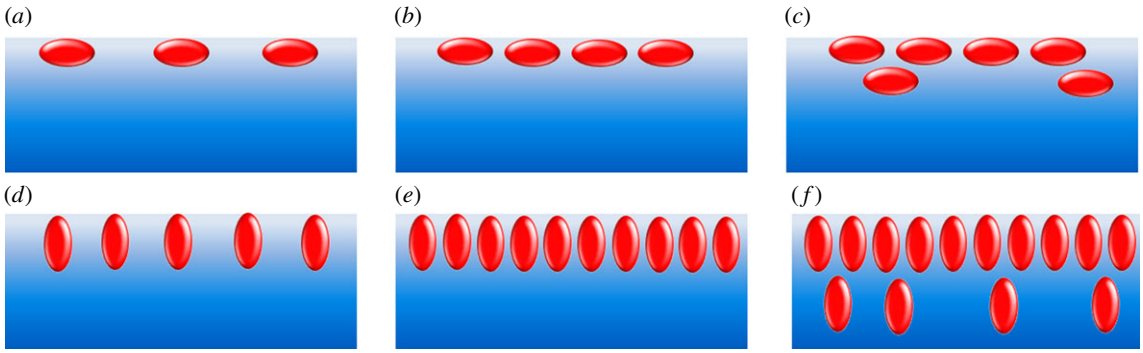


**Figure 6.** Scheme of conceivable BSA arrangements at the air–water interface: (*a*) loosely packed monolayer in a *side-on* orientation, (*b*) closed packed monolayer in a side-on orientation, (*c*) the same as (*b*) having an additional loosely packed second layer, (*d*), (*e*) and (*f*) represent the orientations of (*a*), (*b*) and (*c*) in *edge-on* orientation, respectively. Reprinted from [124], Copyright 2003, with permission from Elsevier. (Online version in colour.)

conformational differences of BSA over a broad pH range around the equilibrium surface pressures [126]. At different pH values and temperatures, BSA and β-lactoglobulin mixed monolayers have been evaluated using compression experiments revealing an electrostatic character of the interaction between the proteins [127]. Desorption phenomena during compression have to be considered evaluating the intermolecular forces.

The understanding of the adsorption behaviour of proteins at the interface has been investigated using BSA with sum-frequency generation (SFG) and ellipsometry [128]. The layer thickness of adsorbed BSA reaches its maximum value close to the isoelectric point, revealing the formation of an amorphous multilayer. At the same pH value, SFG amplitudes show a minimum in the BSA and $H_2O$-related bands, which are attributed to the absence of the electric field at the interface at this pH value. Recent developments using SFG for studying different protein layers (BSA, lysozyme and β-lactoglobulin) at air–water interfaces have been summarized under consideration of the interpretation of SFG spectra [129].

The effect arising from different BSA concentrations or denaturation on the adsorption behaviour, the surface tension is investigated by tensiometry, ellipsometry and IRRAS [124]. The steady-state surface tension of 50 mN m$^{-1}$ (water) is basically independent of concentration but decreases dramatically after thermal denaturation (40 mN m$^{-1}$) caused by different hydrophobicities. Ellipsometry and IRRAS revealed a higher surface density and layer thickness (up to 16 nm) with increasing concentration. Ellipsometry (change in the thickness 9–16 nm and refractive indices 1.42–1.39) and IRRAS support the assumption that at higher concentrations a second BSA layer is formed.

The amino acid sequence of BSA and HSA, which share 76% sequence homology, has no major impact on the overall range of surface excess ($\tilde{A}$). This is related to the surface area, the Avogadro's constant ($\tilde{A} = 1/A\,N_a$) and the thickness of the layers [130]. For HSA, the extrapolated surface area at the zero surface pressure is in the range of 1 m$^2$ mg$^{-1}$ [131]. The $\pi$-$A$ isotherm exhibits a pseudo-plateau between 19 and 24 mN m$^{-1}$, which is attributed to a change from an unfolded to a coiled conformation. BAM investigations reveal very small bright circular domains at low surface pressures ($\pi = 2.5$ mN m$^{-1}$), which grow by compression and form grouping rows ($\pi > 19.2$ mN m$^{-1}$) in the pseudo-plateau region caused by the packing of 'loop' structures. The relative film thickness $d$ increases slowly under compression until $\pi = 15$ mN m$^{-1}$. At higher surface pressures, the fast increasing of d corresponds to packing of the 'loops' achieving a maximum value of 4 nm.

The structure of BSA and HSA monolayers adsorbed at the air–water interface has been studied by neutron specular reflection [130,132]. The surface excess $\Gamma$ increases sharply with increasing concentration where $5 \times 10^{-2}$ g dm$^{-3}$ tends to be the respective saturation limit at pH values close to the isoelectric point. The determined protein layer thicknesses are in the range of the short axial length of the globular protein solution structure (40 Å) over almost all investigated conditions, suggesting an adsorption of the molecules with their long axes parallel to the water surface. The macroscopic film morphology and the spreading dynamics of the defatted form of HSA have been investigated by ellipsometry, neutron reflectometry, X-ray reflectometry and BAM, revealing an alteration from a loose network to a more homogeneous film with increasing concentration [133].

The *in situ* conformational changes in protein layers (β-casein, BSA, lysozyme and fibrinogen) at the air–water interface have been investigated by circular dichroism (CD) spectroscopy technique. The existing α-helices of BSA in solution vanished at the air–water interface and a disordered protein layer is formed. Lysozyme and fibrinogen, being α + β-type proteins in solution, exist in β-sheet conformation at the air–water interface [134].

The fibril formation in BSA and human insulin (HI) monolayers has been evaluated by epifluorescence microscopy at the air–water interface as a faster, cheaper and easier to use alternative to CD spectroscopy and AFM [135]. Time-dependent $\pi$-$A$ isotherm characterization reveals a shift of the lift-off point to smaller surface areas (from 3000 to 2500 Å$^2$) within 48 h, indicating a slightly decreased fibrillization.

The BSA unfolding is studied by dilational surface rheology at the interface using guanidine hydochloride (G.HCl) to determine the critical denaturant concentration [126]. Low concentrations of G.HCl (less than or equal to 0.2 M) lead to a decrease in the electrostatic adsorption barrier. Increasing G.HCl concentrations result in changes in the shape of the dynamic surface elasticity curves due to the formation of loops and tails in the surface layer. The maximum of the dynamic surface elasticity indicates the destruction of the tertiary and secondary structures of BSA at the interface, which takes place at lower concentrations compared to the bulk phase. The unfolding process leads to a re-spreading of the macromolecules requiring a larger surface area. BSA transferred at 10 mN m$^{-1}$ yields a homogeneous layer of protein particles with a diameter of 25 nm and a height of below

5 nm [119] representing the individual molecules ($4 \times 4 \times 14\ nm^3$) [123]. BSA and glutaraldehyde (GA)-treated BSA layers at the air–water interface have been transferred to a solid substrate regarding the ability to react with A-β-galactosidase [136]. The change in the absorbance for GA-treated BSA layer reveals the formation of an antibody film at the surface.

### 3.2.2. Other proteins

The addition of ionic surfactants has a strong impact on the kinetic dependence of the dynamic surface properties, as shown for β-casein [137]. The hydrophilic and hydrophobic parts of β-casein form loops and tails at the interface, while for β-casein/ionic surfactant mixtures the β-casein is displaced from the adsorption layer. Fibronectin (FN) is a glycoprotein of the ECM, which facilitates the binding of cells. The impact of $Ca^{2+}$ and $Na^{+}$ ions and the pH value on a fibronectin monolayer is compared to the monolayer behaviour of bovine submaxillary mucin (BMS) [138]. The specific molecular area is unchanged for BMS by alteration of the ionic strength, but, for fibronectin, the specific molecular area increases linearly with the square root of the ionic strength. The behaviour of FN is attributed to an unfolding structure due to the diminished electrostatic intramolecular interaction. Both proteins exhibit a change in the specific area depending on the pH value.

FN monolayers of high molecular cohesion with defined surface density have been transferred onto polydimethylsiloxane (PDMS) substrates by the LS-method to improve stem cell adhesion behaviour [139]. LS layers are shown to be uniform and homogeneous as indicated by AFM and immunofluorescence images, whereas layers prepared by solution deposition method are rather heterogeneous with the appearance of resembling protein aggregates. Owing to the well-defined organization of the FN LS layers, human mesenchymal stem cells seeded on PDMS showed a reduced absolute number of adherent cells, but a higher and more homogenously vinculin expression in comparison with a PDMS surface equipped with a solution deposition layer, indicating a more *in vivo* like behaviour.

Lysozymes form stable and homogeneous layers at the air–water interface, which can be adjusted by the pH value and the salt concentration [140]. The protein adsorption rate decreases with increasing the positive charge of lysozyme [141]. The equilibrium time period depends on the subphase ion in the following order: buffer < water < saponite dispersion. The homogeneity of the layer is proved by $\pi$-$A$ isotherms, UV-vis and fluorescence spectroscopy [123]. In time-dependent experiments, a decrease in the surface pressure from 0 to $-1\ mN\ m^{-1}$ during the first hour is attributed to the solubility of the lysozyme molecules or exchanges with subphase components. Afterwards, $\pi$ increases within 3–10 h reflecting the formation of a monolayer.

The effect of Hofmeister anion (NaX, X = I, Br, Cl, F) on the adsorption kinetics of the positively charged lysozyme (below the isoelectric point of 11.35) is evaluated by surface tension measurements and time-resolved X-ray reflectometry [141]. The presence of salt increases the protein adsorption rate following an inverse Hofmeister series caused by the interaction of strongly polarized halide anion Br- with the local electric field of the layer which is not the case for $F^{-}$. The initially adsorbed lysozyme molecules have a flat unfolded structure on a pure water subphase. Adding salt leads to the unfolding of the lysozyme molecules during adsorption as a result of protein–protein rearrangements in the following order $F^{-} < Br^{-} \approx I^{-} < Cl^{-}$.

External reflection FTIR spectroscopy has been used to investigate and to compare the conformational changes of three globular proteins, lysozyme, BSA and β-lactoglobulin, adsorbed at the air–water interface [142]. The surface pressure kinetics of the lysozyme adsorption is relatively slow, equilibrium surface pressure is reached after about 2.5 h, while the secondary structure alters within 10 min. Lysozymes form network-like adsorbed structures of unfolded protein layers composed of high content of antiparallel β-sheets. The structural change and the slow gradual adsorption rate are caused by hydrophobic interactions and are associated with a preferred adsorbed orientation or changes in the protein structure.

By contrast, the native structure of BSA and β-lactoglobulin remains stable after the fast adsorption (equilibrium time approx. 10 min) to the interface, which is probably the reason for their higher emulsion efficiency.

The interfacial rheological properties, the protein conformation, and the interaction between adsorbed proteins are reviewed for a variety of proteins such as casein, ovalbumin and β-lactoglobulin [143,144]. For several positively and negatively charged proteins, it has been shown that the adsorption kinetics are strongly influenced by the energetics of interaction of proteins with the interface and not only diffusion-controlled [145]. In general, positively charged proteins exhibit adsorption rates, which are an order of magnitude slower than their respective bulk diffusivities due to the energy barrier for adsorption on the surface. In contrast, for negatively charged proteins the adsorption rates are in the same range than their bulk diffusivities due to their attraction towards the air–water interface. X-ray and neutron reflectometry measurements revealed that adsorbed β-lactoglobulin keeps its globular structure and forms monolayers at the interface (layer thickness 36 Å) [146].

AFM investigations of LB films reveal that the monolayers of lysozyme are homogeneously composed of small, soft round aggregates with a diameter of 25 nm and a height of below 3 nm when transferred at $5\ mN\ m^{-1}$ [123].

### 3.2.3. Peptides

Besides proteins or enzymes, a variety of oligopeptides and polypeptides have been investigated at the air–water interface [44,147,148]. Because of the complexity, only a few examples related to oligopeptides and polypeptides are mentioned here. A more detailed summary of the interactions of β-amyloid-, antimicrobial-, fusion peptides and peptides responsible for protein interaction with membranes has recently been published [32]. Rod-like α-helical polypeptides based on poly-γ-alkyl-L-glutamate form aggregates at the air–water interface during spreading [149,150]. With increasing surface density, poly-γ-benzyl-L-glutamate (PBLG) forms solid-like films with increasing fibre diameters [150]. Moreover, the morphological variation of a stimuli-responsive elastin-like polypeptide (ELP) is investigated as a function of temperature and compression [151]. Stable ELP layers are formed at the air–water interface, whereby an increasing temperature induces a shift of the isotherm to larger surface areas indicating a phase transition followed by the formation

of aggregates. The temperature changes of the secondary structure are investigated by surface-enhanced Raman (SERS) scattering and with atomic force microscopy for LB layers. By circular dichroism (CD) spectroscopy, it is shown that a temperature increase from 21.5°C to 41.5°C leads to the formation of a plateau region in the $\pi$-*A* isotherm caused by a change in the helix orientation [152]. Based on the results obtained from $\pi$-*A* isotherm, CD spectroscopy and AFM, a structural model is derived where the horizontally oriented helices partially alter their orientation to vertical upon compression in the plateau region.

The most important pharmaceutical peptide for diabetes treatment is insulin. To understand the physical/chemical properties of insulin at interfaces, the investigation of its aggregation behaviour is important. The recent progress in this field is summarized for different interfaces focusing the Langmuir technique [153]. Shortly, insulin forms homogenous layers at the air–water interface after spreading on a pure subphase, which is loosely packed before compression. No aggregates are observed by BAM and fluorescein isothiocyanate-labelled insulin epifluorescence [154]. Moreover, zinc concentration, pH, ionic strength, and proteins in the subphase lead to aggregation of insulin at the air–water interface. Spread from acid solution insulin forms homogeneous layers at 20°C [154]. Acidic pH values (pH = 1) result in a more expanded conformation compared to pH 5.7, indicating the presence of an increased amount of monomeric insulin. By contrast, association of insulin molecules has been observed at pH 10 forming a more compact and rigid monolayer with smaller mean molecular surface area.

The human insulin (HI) Langmuir monolayers are investigated in the presence and absence of Zn(II) ions depending on the subphase pH value, revealing different conformation by spectroscopic data [153,155]. The addition of zinc ions influences the lifting up of the molecular surface area and the transition state [156]. Surface pressure–area and surface potential-area isotherms suggest aggregation of the HI molecules at the air–water interface in the presence of Zn(II) ions [155]. Infrared absorption and CD spectroscopy reveal a higher content of β-sheet and β-strands, as aggregation occurred under basic conditions. Compression–decompression cycles show that the HI aggregates are not stable and tend to spread to a monomolecular monolayer, which is in accordance with UV-vis and fluorescence spectroscopy analysis. IRRAS obtained mainly α-helix and less β-sheet structures at different surface pressures; however, the spectral bands differ from those obtained in solution. Reasons for the conformational change of the insulin probably are a lower degree of freedom of the molecules and misfolding of the hydrophobic residues and their exposing to the air, while the hydrophilic segments submerge into the subphase.

## 4. Polymer–protein interactions at the air–water interface

The Langmuir technique proved to be a powerful tool for the investigation of *in situ* molecular interaction between the surface layer and subphase compounds. The interaction between polymer and biomolecules leads to functional changes of the material–environment interface. Such modification can be investigated by applying the Langmuir monolayer approach. For example, the surfaces of a spin-casted PLA film, functionalized by LB-layers of amphiphilic AB or ABA block copolymers of PLA as A block and either PEO, α-methoxy-ω-hydroxy PEO, α-carboxy-ω-hydroxy PEO or poly(L-aspartic acid) as B block, improve the protein and cell adhesion [157]. The simulation of the biomolecule impact, such as proteins or enzymes, on a pre-existing synthetic polymer layer is discussed in this section on the microscopic and macroscopic level.

PLA is often used in medical applications and for tissue regeneration [158,159]. Its hydrophobic character is the reason for non-specific protein adsorption. The modification of the interfacial properties of PLA has been shown using Langmuir monolayer technique by applying mixed monolayers with hydrophilic PEO-polypropylene oxide triblock copolymers (PEO-*b*-PPO-*b*-PEO) [160]. Thus, the interaction with BSA molecules (adsorbed/penetrated) at the air–water interface of the PEO-*b*-PPO-*b*-PEO-modified-PLA monolayer is tuned by changing the surface density and chain length of PEO. The hydrophilization with long PEO segments reduces the protein adsorption compared to pure PLA monolayers due to the formation of a thick (twice as thick as a radius of gyration $R_G$) PEO layer immersed into the subphase.

The formation of poly(styrene)-*b*-poly(ethylene oxide) (PS-*b*-PEO) monolayers inhibits the HSA adsorption to the air–water interface [161]. The layer thickness of PS-*b*-PEO monolayer in the presence and absence of albumin is determined by *in situ* surface plasmon resonance (SPR) measurements. The closed packed PEO 'brushes' operate as a shield and prevent albumin adsorption. An effective inhibition is obtained only after the formation of brush-like structures, as illustrated in figure 7. At lower PEO surface density, the surface pressure kinetics of albumin insertion reveals two different situations: albumin binds to the air–water interface very rapidly when PEO is below the 'pancake-brush' transition and is able to induce this transition. Above the transition, albumin penetrates in between free spaces of the PS-*b*-PEO monolayer.

Mixed monolayers based on PLA50 and BSA are studied to evaluate the film organization considering composition and compression state, whereas the influence of each component is successfully described by the Maxwell's model [162]. Up to approximately 15 mN $m^{-1}$ (phase transition), the shape of the isotherm is governed by PLA50. During the phase transition of PLA50, a continuous BSA phase is formed from then on defining the rheological properties of the monolayer. AFM of corresponding LB films transferred at 16 mN $m^{-1}$ shows separate aggregates on a homogeneous layer, suggesting a condensed PLA50 phase. Langmuir and LB experiments suggest that BSA molecules are present between PLA50 aggregates, preventing the interaction of the polyester molecules [76].

Concerning the degradation of polymer layers at the air–water interface, the interaction of polymer layers with enzymes and degradation fragments is a major topic. It is assumed that degradation fragments immediately dissolve into the subphase and have not been considered in the degradation process anymore. Recently, the impacts of the intermediate hydrolysis products of PLGA consisting of both water-soluble and water-insoluble components have been investigated [163]. Monolayers based on water-insoluble degradation OLGA fragments reveal highly compressible film behaviour, which significantly differs from the complex behaviour observed for pristine PLGA. An increased

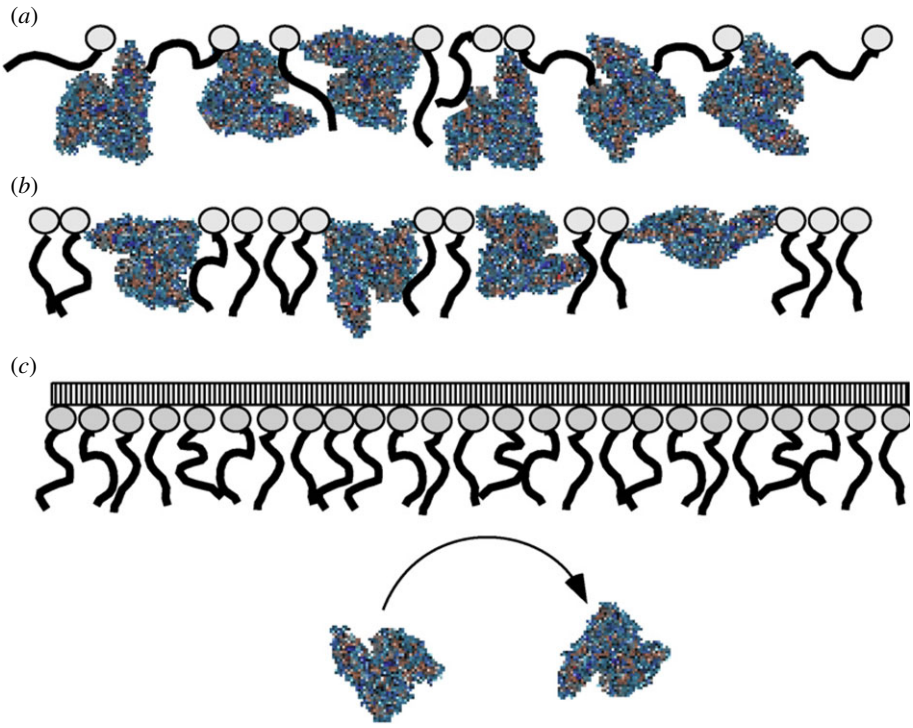


**Figure 7.** Possible description of the HSA penetration into a PS-*b*-PEO monolayer at different surface densities (*a*) at low packing density of PS-*b*-PEO: HSA easily penetrates into the monolayer, (*b*) medium packing density of PS-*b*-PEO: the HSA adsorption leads to a pancake–brush-transition and (*c*) high packing density of PS-*b*-PEO: PEO brushes inhibit HSA penetration. Reprinted from [161], Copyright 2007, with permission from Elsevier. (Online version in colour.)

elasticity modulus of the Langmuir layer is obtained as a consequence of improved packing abilities and increased water-solubility. Water-soluble degradation fragments are surface-active. On the contrary, lactic acid and glycolic acid do not influence the surface tension of water, but are able to form weakly interacting by H-bonds reducing the required monolayer surface area by looping effect in combination with a PLGA layer.

## 5. Langmuir monolayer degradation of polymer layers

### 5.1. General principles

Biodegradation of polymers is usually observed by time-consuming *in vitro* or *in vivo* methods using three-dimensional samples considering diffusion processes for the evaluation of the degradation kinetics. Using Langmuir monolayer methods, all polymer chains are in direct contact with the air–water interface. Therefore, diffusion processes of the degrading components (like water) in the surrounding fluid and the degradation fragments out of the sample are excluded as kinetically relevant. By applying the Langmuir monolayer degradation (LMD) technique, the hydrolytic as well as enzymatic degradation of polymers can be investigated. Degradation conditions can easily be varied (temperature, pH value, enzyme addition, salt type and concentration) allowing a versatile access to the degradation properties of plenty of different materials. In this section, the degradation of polymer layers at the air–water interface is considered.

During LMD experiments, the reduction of the covered surface area with time is recorded under constant surface pressure (barostatic) conditions. The experimental setup for an enzymatic degradation experiment is shown in figure 8. In the first step, a closed packed monolayer is formed by compression of the polymer film, which is typically the case at the inflection point of the $\pi$-$A$ isotherm. The hydrolysis of esters, amides or other bonds in the polymer main chain results in the formation of water-soluble low molecular weight fragments (oligomers and monomers), which are able to leak out of the polymer monolayer into the subphase. To keep the surface pressure constant, the surface area has to be decreased as a result of the reduced amount of molecules at the interface. This time-dependent surface area reduction indicates the degradation process of the polymer. The depiction of the area reduction versus the time is called degradation curve, allowing the correlation between the reduction of the covered surface area and the formation of water-soluble molecules. Different descriptions are used for the surface area reduction data. In a simplified way, the surface area reduction is represented only by dividing the covered surface area ($A_t$) after the degradation time interval t by the initially required surface area of the compressed monolayer ($A_0$) [164]. Alternatively, the surface area reduction is described by the total area loss ($\Delta A(t)$) at a certain time point where $\Delta A(t)$ is the difference between $A_0$ and $A_t$ [165]. Based on this, the relative area change $\Delta A_{\mathrm{rel}}(t)$ is given as follows:

$$\Delta A_{\mathrm{rel}}(t) - (A_0 - A_t) \cdot A_0^{-1}. \tag{5.1}$$

Applying the dynamic fragmentation model, the corrected surface area reduction ($\Delta A_{\mathrm{corr}}(t)$), calculated according to equation (5.2), $\Delta A_{\mathrm{rel}}(t)$ is often used for the description of the degradation kinetics. This model considers the correction of small surface areas value [166].

$$\Delta A_{\mathrm{corr}}(t) = \Delta A_{\mathrm{rel}}(t) \cdot (A_0 \cdot A_t^{-1}) = (A_0 \cdot A_t^{-1}) - 1. \tag{5.2}$$

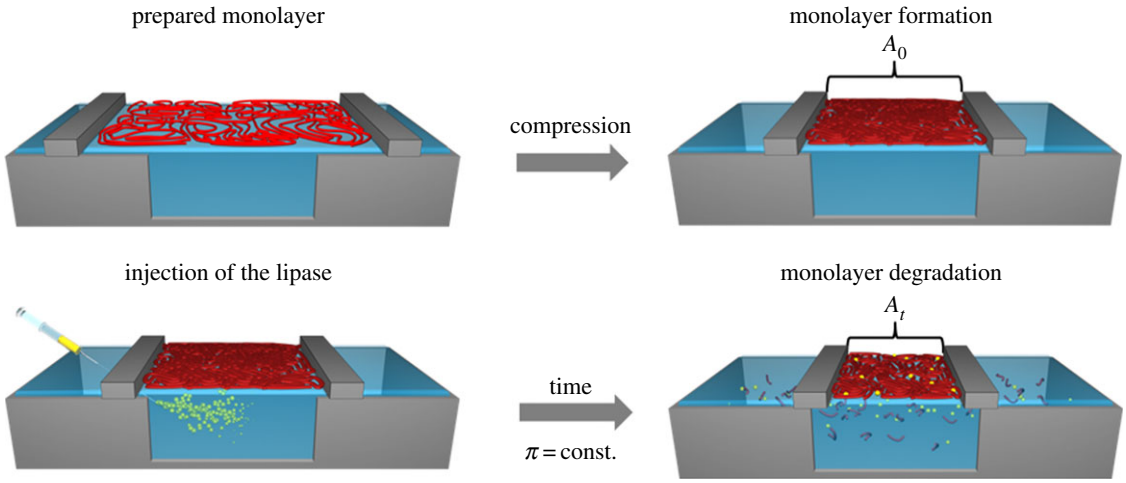


**Figure 8.** Schematic of the implementation of an LMD experiment at the air–water interface: monolayer formation by compression, injection of the enzyme into the subphase beneath the monolayer and monolayer degradation by fragmentation under constant surface pressure conditions. $A_0$ and $A_t$ correspond to equation (5.2).

By applying this modelling approach, two degradation mechanisms can be distinguished based on the characteristic release kinetics of water-soluble degradation fragments leaving the air–water interface into the subphase: random chain scission and chain-end cut mechanism [166].

In analogy to the bulk degradation, random chain scission is characterized by an exponential slope, and chain-end scission mechanism by linear slope (figure 9) [167,168]. Considering the bond cleavage mechanisms of macromolecules at the air–water interface, the hydrolytic degradation and enzymatic degradation play the most prominent role. Therefore, the kind of polymers, which are applicable for the monolayer degradation approach is limited, and most established examples belong to the family of polyesters, like PLA- and PCL-based (co)polymers.

## 5.2. Langmuir monolayer degradation investigations of polyester-based monolayers

The degradation of polyesters and blended polyesters monolayers has been analysed with an emphasis on the composition, the degrading medium and its pH value. A sigmoid-shaped degradation curve is obtained for the hydrolytic degradation of *rac*-PLA monolayers using the change of surface area ratio ($A/A_0$) on an alkaline subphase (pH = 10.5) [169]. Moreover, the extent of surface area ratio reduction increases with increasing surface pressure ($\pi = 4$, 7, 10 mN m$^{-1}$). Under alkaline conditions, an instantaneous linear surface area reduction is obtained in LMD experiments ($\Delta A_{corr}(t)$) revealing a chain-end scission mechanism for *rac*-PLA and PLGA [165]. These results are supported by three-dimensional degradation investigations of oligolactides terminated with hydroxyl functions, which are preferably hydrolytic degraded by a backbiting mechanism [170].

Alkaline pH values of the subphase are necessary to increase the degradation velocity in a time period suitable for the Langmuir technique in the case of PLA. At acidic pH values (pH 1.9 and 3.5), no degradation is observed within a time range of 100 min [169,171]. Particularly, for PLA-based materials, the specification of the stereochemistry has a comprehensive effect on the biological and physical properties. Three- and two-dimensional degradation reveals a significant faster degradation of amorphous *rac*-PLA compared to the semi-crystalline PLLA and PDLA [172,173]. Moreover, reduced hydrolysis rates of PLLA/PDLA stereocomplexes arise from a higher degree of crystallinity as well as a stronger interaction in the formed stereocomplex compared to PLLA homopolymer [174]. Stereocomplex formation in enantiomeric PLA Langmuir monolayers also causes stereo-selective enzymatic degradation by proteinase K [173], where equimolar mixed monolayers of PLLA and PDLA blends degrade substantially slower compared to its homopolymers. The blending of crystallizable polymers like PLLA and PCL results in a faster degradation of the layer revealing the importance of the orientation and crystallization behaviour [164,175]. In blends, the hydrolysis is enhanced by the decreased order of the chains in the monolayer. The two-dimensional enzymatic hydrolysis of PLA-*co*-PEO occurs with constant hydrolysis rates in accordance with the random fragmentation mechanism predicted for PLA. Accumulation of charged, water-insoluble PLA fragments is detected by surface potential measurements [176]. Considering the uniqueness of polymers, it is obvious that the degradation velocity depends on their molecular weight. For low molecular weight polymers, the surface area reduction occurs faster due to the faster formation of water-soluble degradation fragments, which has been confirmed for PLA- and PCL-based Langmuir monolayer in accordance with three-dimensional degradation studies [165,177]. For PCL-based monolayers, the largest water-soluble degradation fragments are tetramers [178].

The hydrolytic chain scission rate of random PLGA copolymers increases compared to *rac*-PLA at the air–water interface due to the introduction of more hydrophilic PGA units as it is known from bulk investigations [171,179]. In contrast, the slightly more hydrophobic poly-(*R*)-3-hydroxybutyrate (P3HB, composed of an additional $CH_2$-group per monomer unit) forms more hydrolytically stable monolayers [180,181], which is attributed to a reduced submerging of the polymer chains into the subphase. The access of the functional units defines the ability of interaction between polymer backbone and a biomolecule regarding the degradation behaviour as well as for adsorption studies. In two-dimensional enzymatic degradation studies of P3HB and PLA, a reduced enzymatic degradation velocity compared to alkaline degradation is the result of a lower accessibility of the functional units caused by the large size of the enzyme compared to the alkaline ions [180]. The

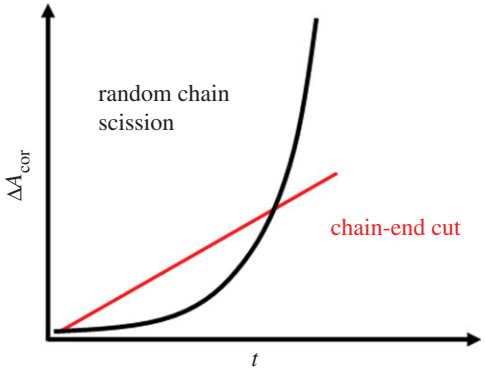


**Figure 9.** Schematic of two-dimensional degradation curve by random chain scission and chain-end cut mechanism. (Online version in colour.)

PCL backbone is more hydrophobic compared to PLA and P3HB, which results in significant longer hydrolytic degradation times [164,175,182], but the enzymatic degradation is accelerated by a variety of enzymes [178,183,184]. A random chain scission of the PCL chains has been obtained at the air–water interface using the lipase from *Humicola lanuginosa* and the lipase from *Pseudomonas cepacia* [166,178,185]. Surface potential measurements reveal charged degradation fragments at the interface [178].

The degradation behaviour of PCL is modified by the introduction of enzymatic non-degradable (related to the lipase from *Pseudomonas cepacia*) segments. The multiblock copolymers (PDC) composed of PCL and PPDO segments linked by TMDI reveal an almost linear weight loss, which is described by a random chain scission process using a dangling chain model [108]. The enzymatic degradation of the PCL segments proceeds faster compared to the hydrolytic bond cleavage in the PPDO blocks. By changing the chemical composition (the ratio of PPDO to PCL segments), the degradation rates are adjusted in two-dimensional as well as in three-dimensional degradation experiments [186]. Regarding the enzymatic degradation of copolymer-based monolayers composed of degradable and of hydrophobic, non-degradable segments, the polymer–enzyme interaction behaviour has to be considered. Using the example of multiblock copolymers, PDLCL constituted of oligo(ε-caprolactone) (OCL) segments and the hydrophobic oligo(ω-pentadecalactone) (OPDL) segments, which are non-degradable by this specific lipase from *P. cepacia* (figure 10). The introduction of a hydrophobic segment (OPDL) reduces the degradation rates of PCL-based multiblock copolymers (PDLCL) as a result of polymer–enzyme interactions [187]. At the beginning, the copolymer forms a homogeneous layer consisting in equal shares of OCL and OPDL segments requiring the surface area $A_0$. With ongoing time, the amount of OCL fragments at the interface decreases due to the formation of water-soluble OCL degradation fragments by enzymatic bond cleavage. As OPDL cannot be degraded by the lipase from *P. cepacia*, a defined surface area has to remain ($A_r$) after the entire degradation of the OCL segments. Moreover, the surface-active lipase is able to interact with the non-degradable OPDL segments. Therefore, $A_r$ is the sum of the required surface area of OPDL segments and the surface-active lipase. The enrichment of lipase at the polymer–water interface induces morphological changes expanding the required surface area of the polymer layer [187]. Consequently, the surface area versus time correlation of the PDLCL monolayer consists of the induced change of the required surface area due to the polymer–enzyme interactions (OPDL segments) and the formation of water-soluble degradable fragments (OCL segments).

In contrast to PPDO segments, the OPDL segments stay at the air–water interface independent of the degree of degradation of the OCL segments enabling unrestricted interaction with the surface-active lipase decreasing the apparent surface area reduction. While the PPDO segments promote the surface area reduction in PDC, for PDLCL the formation of water-soluble fragments is reduced, since small OCL degradation fragments, not connected to OPDL segments, can be solved in the subphase only.

For the degradation mechanism as well as for the interaction with other molecules in the subphase, the influence of the end groups is an important topic in three- as well as in two-dimensional systems. Functional end groups, for example, can act as linker units and therefore support/prevent adsorption of molecules to the interface due to sterically hindrance or hydrophilic/hydrophobic interaction/repulsion, respectively. For PLA monolayers based on end-capped and non-end-capped polymers, the same degradation rates are obtained revealing the influence of transport process in bulk degradation investigations, which can be neglected in two-dimensional systems [165]. End-capped OCL with phenylboronic acid pinacol ester or phenylboronic acid are investigated using the LMD technique regarding the enzymatic degradation behaviour [188]. While the layer compression behaviour of end-capped OCL layers is less affected, the injection of the lipase from *P. cepacia* leads to a retarded film degradation compared to pure OCL layers by incorporation of the enzyme molecules into the layer due to end group effects.

Besides hydrophilicity and end groups, the polymer architecture affects the degradation behaviour. Using star-shaped PCLs, the overall hydrophilicity is increased, while the molecular weight is constant [189]. The increase of the hydrophilicity of star-shaped polymers has an impact on the chain packing behaviour and therefore on the degradation behaviour of the monolayer. Moreover, the chain scission by the lipase from *P. cepacia* is prevented by the introduction of randomly distributed urethane linkers in the PCL chain.

## 6. Summary and outlook

This article provides an overview of the capabilities of Langmuir techniques for elucidating the polymeric biomaterial–environment interface. It is focused on polymer films at the air–water interface to study the interaction with proteins as well as the ability of proteins to form Langmuir or Gibbs layers interacting with other substances in the subphase. The Langmuir monolayer technique reveals a high potential for investigating both morphological and degradation behaviour of natural and synthetic polymers, evolving several of new attractive topics. The interfacial properties of polymers are significantly influenced by their composition and architecture, which determine crystallization and aggregation processes. The Langmuir monolayer degradation technique provides monomolecular layers at the interface, which allows their investigation excluding diffusion processes. The LMD approach refers to the formation of water-soluble degradation fragments, based on bond cleavages in the polymer backbone and their submerging of low molecular weight

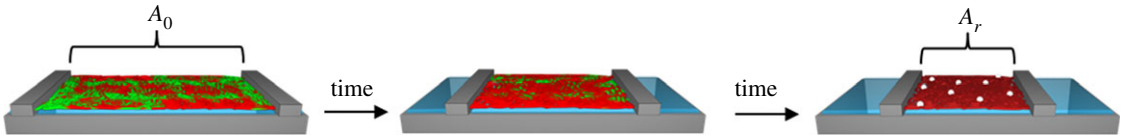


**Figure 10.** Depiction of the PDLCL degradation at the air–water interface as a result of two parallel processes: film degradation (green OCL segments) and polymer–enzymes interaction (red OPDL segments). The enzyme is represented by the white bullets.

fragments into the subphase. The impact of hydrophilic water-insoluble segments on the surface area reduction is also accessible. Thereby, the degradation conditions can be varied allowing a versatile access to the hydrolytic and enzymatic degradation properties of plenty of different polymers. Moreover, the Langmuir approach enables the parallel analyses of both the polymer–biomolecule interactions and the degradation process at the molecular level. The interactions between the polymer material and its degradation products influencing its degradation behaviour are exhibited by the Langmuir technique.

For future investigations, a variety of surface-specific spectroscopic and microscopic techniques are available to gain new information on orientation, packing motifs and intermolecular interactions. For example, IRRAS, which has so far only been performed for a limited number of proteins and synthetic polymers, could provide access to structural and orientational changes. Moreover, degradation processes and hydrolysis kinetics of monolayers are accessible and can occur without the formation of water-soluble degradation fragments. The enrichment of surface-active degradation products and water-soluble proteins/enzymes at the pure or covered surface can be monitored providing information about real-time conformational changes related to interactions with surface-active enzymes and absorption kinetics.

A key challenge is the identification of water-soluble degradation fragments and the determination of the concentration in the subphase due to their low concentration. Electrospray ionization mass spectrometry (ESI-MS) may allow the determination of fragment traces giving new insights into the interactions of water-soluble molecules and polymer layers degradation processes. Chemical changes in the monolayer during degradation without the formation of water-soluble fragments can be identified by the shape and position of the IR bands corresponding to the stretching and deformation vibrations. Besides IRRAS, surface potential measurements provide access to the enrichment of water-insoluble and surface-active subphase components.

Rheological properties of the Langmuir layer got recently into special interest. The investigation of interfacial rheology is applied to understand the viscoelastic properties, which provide the modulus and relaxation behaviour [190] and to gain information about the structure–rheology interplay. The two-dimensional properties for a variety of systems like synthetic (co)polymers [115,191,192], mixed protein layers [193], biomolecules [45,194,195] and low molecular weight molecules [196] have been performed. However, investigations on pure protein layers and their interaction with water-soluble molecules are still challenging. The degradation kinetics as well as the adsorption kinetics of degradation fragments has to be understood in more detail for future applications of polymer-based biomaterials. More detailed information about the molecular arrangement is provided by spectroscopic ellipsometry (layer thickness) and *in situ* synchrotron X-ray scattering methods, which enable the evaluation of crystalline regions.

To judge experimental data and to gain a complete understanding at the monomolecular level, computer simulation studies are required including molecular dynamic and quantum chemical analyses applied in combination with the results obtained in Langmuir investigations, as it has been done for the hydrolytic degradation of polymer-based biomaterials [197]. This knowledge-based approach is required to enable the tailored design of biodegradable polymeric materials.

The combination of a variety of analytical methods, including microscopy, spectroscopy and scattering techniques, with the Langmuir technique applied on polymers and biomolecules is challenging, but opens a tool box, which will provide new insights for the evaluation of biomaterial interface science. Conclusively, the described Langmuir techniques together with improved analytical methods cannot only be used for fundamental investigation of the polymer behaviour on the air–water interface, but may also be applicable for investigation that aim to understand the *in vivo* behaviour of polymers and their interaction with proteins.

Authors' contributions. A.-C.S., T.R., B.S. and A.L. wrote the review article.

Competing interests. We declare we have no competing interests.

Funding. The authors thank the Helmholtz Association for partially funding through programme-oriented funding and grant no. VH-VI-423 (Helmholtz Virtual Institute, Multifunctional Biomaterials for Medicine).

## References

1. Williams D. 2014 *Essential biomaterials science*. Cambridge, UK: Cambridge University Press.
2. Rydz J, Sikorska W, Kyulavska M, Christova D. 2014 Polyester-based (bio)degradable polymers as environmentally friendly materials for sustainable development. *Int. J. Mol. Sci*. **16**, 564–596. (doi:10.3390/ijms16010564)
3. Kohane DS, Langer R. 2008 Polymeric biomaterials in tissue engineering. *Pediatr. Res*. **63**, 487–491. (doi:10.1203/01.pdr.0000305937.26105.e7)
4. Campoccia D, Montanaro L, Arciola CR. 2013 A review of the biomaterials technologies for infection-resistant surfaces. *Biomaterials* **34**, 8533–8554. (doi:10.1016/j.biomaterials.2013.07.089)
5. Gupta B, Revagade N, Hilborn J. 2007 Poly(lactic acid) fiber: an overview. *Prog. Polym. Sci*. **32**, 455–482. (doi:10.1016/j.progpolymsci.2007.01.005)
6. Ulery BD, Nair LS, Laurencin CT. 2011 Biomedical applications of biodegradable polymers. *J. Polym. Sci. B Polym. Phys*. **49**, 832–864. (doi:10.1002/polb.22259)

7. Liang Y, Li L, Scott RA, Kiick KL. 2017 50th anniversary perspective: polymeric biomaterials: diverse functions enabled by advances in macromolecular chemistry. *Macromolecules* **50**, 483–502. (doi:10.1021/acs.macromol.6b02389)
8. Ha TLB, Quan TM, Vu DN, Si DM. 2013 Naturally derived biomaterials: preparation and application. In *Regenerative medicine and tissue engineering* (ed. JA Andrades), pp. 247–274. Rijeka, Croatia: InTech.
9. Teo AJT, Mishra A, Park I, Kim Y-J, Park W-T, Yoon Y-J. 2016 Polymeric biomaterials for medical implants and devices. *ACS Biomater. Sci. Eng*. **2**, 454–472. (doi:10.1021/acsbiomaterials.5b00429)
10. Chew SA, Danti S. 2017 Biomaterial-based implantable devices for cancer therapy. *Adv. Healthcare Mater*. **6**, 1600766. (doi:10.1002/adhm.201600766)
11. Zhang X, Cheng J, Zhuo R. 2016 Amphiphilic hyperbranched polymers with a biodegradable hyperbranched poly(ε-caprolactone) core prepared from homologous AB2 macromonomer. *RSC Adv*. **6**, 52 334–52 338. (doi:10.1039/C6RA08531H)
12. Dash TK, Konkimalla VB. 2012 Polymeric modification and its implication in drug delivery: poly-ε-caprolactone (PCL) as a model polymer. *Mol. Pharmaceut*. **9**, 2365–2379. (doi:10.1021/mp3001952)
13. Mondal D, Griffith M, Venkatraman SS. 2016 Polycaprolactone-based biomaterials for tissue engineering and drug delivery: current scenario and challenges. *Int. J. Polym. Mater*. **65**, 255–265. (doi:10.1080/00914037.2015.1103241)
14. Anderson JM. 2001 Biological responses to materials. *Annu. Rev. Mater. Res*. **31**, 81–110. (doi:10.1146/annurev.matsci.31.1.81)
15. Prasad Shastri V, Lendlein A. 2010 Engineering materials for regenerative medicine. *MRS Bull*. **35**, 571–577. (doi:10.1557/mrs2010.524)
16. Unadkat HV *et al.* 2011 An algorithm-based topographical biomaterials library to instruct cell fate. *Proc. Natl Acad. Sci. USA* **108**, 16 565–16 570. (doi:10.1073/pnas.1109861108)
17. Metavarayuth K, Sitasuwan P, Zhao X, Lin Y, Wang Q. 2016 Influence of surface topographical cues on the differentiation of mesenchymal stem cells *in vitro*. *ACS Biomater. Sci. Eng*. **2**, 142–151. (doi:10.1021/acsbiomaterials.5b00377)
18. Saltzman WM. 2000 Cell interactions with polymer. In *Principles of tissue engineering* (eds RP Lanza, R Langer, J Vacanti), 2nd edn. New York, NY: Academic Press.
19. Watson S, Nie M, Wang L, Stokes K. 2015 Challenges and developments of self-assembled monolayers and polymer brushes as a green lubrication solution for tribological applications. *RSC Adv*. **5**, 89 698–89 730. (doi:10.1039/C5RA17468F)
20. Decher G. 2012 Layer-by-layer assembly (putting molecules to work). In *Multilayer thin films* pp. 1–21. Weinheim, Germany: Wiley-VCH Verlag GmbH & Co. KGaA.
21. Saums MK, Wang WF, Han B, Madhavan L, Han L, Lee D, Wells RG. 2014 Mechanically and chemically tunable cell culture system for studying the myofibroblast phenotype. *Langmuir* **30**, 5481–5487. (doi:10.1021/la4047758)
22. Bose S, Keller SS, Alstrøm TS, Boisen A, Almdal K. 2013 Process optimization of ultrasonic spray coating of polymer films. *Langmuir* **29**, 6911–6919. (doi:10.1021/la4010246)
23. Krebs FC. 2009 Fabrication and processing of polymer solar cells: a review of printing and coating techniques. *Sol. Energy Mater. Sol. Cells* **93**, 394–412. (doi:10.1016/j.solmat.2008.10.004)
24. Ariga K, Yamauchi Y, Mori T, Hill JP. 2013 25th anniversary article: What can be done with the Langmuir-Blodgett method? Recent developments and its critical role in materials science. *Adv. Mater*. **25**, 6477–6512. (doi:10.1002/adma.201302283)
25. Giner-Casares JJ, Brezesinski G, Mohwald H. 2014 Langmuir monolayers as unique physical models. *Curr. Opin. Colloid Interface Sci*. **19**, 176–182. (doi:10.1016/j.cocis.2013.07.006)
26. Berry JD, Neeson MJ, Dagastine RR, Chan DYC, Tabor RF. 2015 Measurement of surface and interfacial tension using pendant drop tensiometry. *J. Colloid Interface Sci*. **454**, 226–237. (doi:10.1016/j.jcis.2015.05.012)
27. Wang K-H, Lin W-D, Wu J-Y, Lee Y-L. 2013 Conformation transitions of adsorbed proteins by interfacial forces at an air-liquid interface and their effect on the catalytic activity of proteins. *Soft Matter* **9**, 2717–2722. (doi:10.1039/C2SM27371C)
28. Xu R, Dickinson E, Murray BS. 2007 Morphological changes in adsorbed protein films at the air-water interface subjected to large area variations, as observed by Brewster angle microscopy. *Langmuir* **23**, 5005–5013. (doi:10.1021/la063280q)
29. Chenoweth DE. 1984 Complement activation during hemodialysis: clinical observations, proposed mechanisms, and theoretical implications. *Artif. Organs* **8**, 281–287. (doi:10.1111/j.1525-1594.1984.tb04291.x)
30. Johnson RJ. 1994 Complement activation during extracorporeal therapy: biochemistry, cell biology and clinical relevance. *Nephrol. Dial. Transplant*. **9**(Suppl. 2), 36–45.
31. Shepard AD, Gelfand JA, Callow AD, O'Donnell Jr TF. 1984 Complement activation by synthetic vascular prostheses. *J. Vasc. Surg*. **1**, 829–838. (doi:10.1016/0741-5214(84)90015-6)
32. Nobre TM, Pavinatto FJ, Caseli L, Barros-Timmons A, Dynarowicz-Łątka P, Oliveira Jr ON. 2015 Interactions of bioactive molecules & nanomaterials with Langmuir monolayers as cell membrane models. *Thin Solid Films* **593**, 158–188. (doi:10.1016/j.tsf.2015.09.047)
33. Stefaniu C, Brezesinski G, Möhwald H. 2014 Langmuir monolayers as models to study processes at membrane surfaces. *Adv. Colloid Interface Sci*. **208**, 197–213. (doi:10.1016/j.cis.2014.02.013)
34. Travkova OG, Andra J, Mohwald H, Brezesinski G. 2010 Conformational properties of arenicins: from the bulk to the air-water interface. *Chemphyschem* **11**, 3262–3268. (doi:10.1002/cphc.201000472)
35. Travkova OG, Andra J, Mohwald H, Brezesinski G. 2013 Influence of Arenicin on phase transitions and ordering of lipids in 2D model membranes. *Langmuir* **29**, 12 203–12 211. (doi:10.1021/la402340d)
36. Travkova OG, Brezesinski G. 2013 Adsorption of the antimicrobial peptide arenicin and its linear derivative to model membranes - a maximum insertion pressure study. *Chem. Phys. Lipids* **167**, 43–50. (doi:10.1016/j.chemphyslip.2013.01.010)
37. Rayleigh L. 1889 Measurements of the amount of oil necessary in order to check the motions of camphor upon water. *Proc. R. Soc. Lond.* **47**, 364–367. (doi:10.1098/rspl.1889.0099)
38. Pockels A. 1891 Surface tension. *Nature* **43**, 437–439. (doi:10.1038/043437b0)
39. Kaganer VM, Mohwald H, Dutta P. 1999 Structure and phase transitions in Langmuir monolayers. *Rev. Mod. Phys*. **71**, 779–819. (doi:10.1103/RevModPhys.71.779)
40. Phan MD, Lee J, Shin K. 2016 Collapsed STATES of Langmuir monolayers. *J. Oleo Sci*. **65**, 385–397. (doi:10.5650/jos.ess15261)
41. Kumaki J, Kajitani T, Nagai K, Okoshi K, Yashima E. 2010 Visualization of polymer chain conformations in amorphous polyisocyanide Langmuir-Blodgett films by atomic force microscopy. *J. Am. Chem. Soc*. **132**, 5604–5606. (doi:10.1021/ja908426u)
42. Maestro A, Hilles HM, Ortega F, Rubio RG, Langevin D, Monroy F. 2010 Reptation in langmuir polymer monolayers. *Soft Matter* **6**, 4407–4412. (doi:10.1039/c0sm00250j)
43. Gavranovic GT, Deutsch JM, Fuller GG. 2005 Two-dimensional melts: polymer chains at the air-water interface. *Macromolecules* **38**, 6672–6679. (doi:10.1021/ma050061n)
44. Lhor M, Bernier SC, Horchani H, Bussieres S, Cantin L, Desbat B, Salesse C. 2014 Comparison between the behavior of different hydrophobic peptides allowing membrane anchoring of proteins. *Adv. Colloid Interface Sci*. **207**, 223–239. (doi:10.1016/j.cis.2014.01.015)
45. Caruso B, Ambroggio EE, Wilke N, Fidelio GD. 2016 The rheological properties of beta amyloid Langmuir monolayers: comparative studies with melittin peptide. *Colloids Surf. B* **146**, 180–187. (doi:10.1016/j.colsurfb.2016.06.003)
46. Crawford NF, Leblanc RM. 2014 Serum albumin in 2D: a Langmuir monolayer approach. *Adv. Colloid Interface Sci*. **207**, 131–138. (doi:10.1016/j.cis.2013.10.021)
47. Lopez RF, Nobre TM, Accardo CD, Pernambuco PC, Nader HB, Lopes CC, Caseli L. 2013 Effect of carrageenans of different chemical structures in biointerfaces: a Langmuir film study. *Colloids Surf. B* **111**, 530–535. (doi:10.1016/j.colsurfb.2013.06.039)
48. Toulemon D, Liu Y, Cattoën X, Leuvrey C, Bégin-Colin S, Pichon BP. 2016 Enhanced collective magnetic properties in 2D monolayers of iron oxide nanoparticles favored by local order and local 1D shape anisotropy. *Langmuir* **32**, 1621–1628. (doi:10.1021/acs.langmuir.5b04145)
49. Tsukanova V, Slyadneva O, Inoue T, Harata A, Ogawa T. 1999 Compression of the dye monolayer at the

air/water interface studied by second harmonic generation. *Chem. Phys*. **250**, 207–215. (doi:10.1016/S0301-0104(99)00257-8)

50. Sergeeva TI, Gromov SP, Vedernikov AI, Kapichnikova MS, Alfimov MV, Möbius D, Zaitsev SY. 2005 Organisation in monolayers at the air–water interface of butadienyl dyes containing benzodithiacrown-ether or dimethoxybenzene. *Colloids Surf. A* **264**, 207–214. (doi:10.1016/j.colsurfa.2005.05.024)
51. Bulhoes LOS, Obeng YS, Bard AJ. 1993 Langmuir-Blodgett and electrochemical studies of fullerene films. *Chem. Mater*. **5**, 110–114. (doi:10.1021/cm00025a021)
52. Liu WJ, Jeng U, Lin TL, Lai SH, Shih MC, Tsao CS, Wang LY, Chiang LY, Sung LP. 2000 Adsorption of dodecahydroxylated-fullerene monolayers at the air–water interface. *Phys. B* (*Amsterdam, Neth.*) **283**, 49–52. (doi:10.1016/S0921-4526(99)01890-6)
53. Jin J *et al.* 1999 Structural characterizations of C60-derivative Langmuir—Blodgett films and their photovoltaic behaviors. *Langmuir* **15**, 4565–4569. (doi:10.1021/la981459y)
54. Moon HK, Choi YS, Lee JK, Ha CS, Lee WK, Gardella JA. 2009 Miscibility and hydrolytic behavior of poly(trimethylene carbonate) and poly(L-lactide) and their blends in monolayers at the air/water interface. *Langmuir* **25**, 4478–4483. (doi:10.1021/la8032435)
55. Deschênes L, Lyklema J, Danis C, Saint-Germain F. 2015 Phase transitions in polymer monolayers: application of the Clapeyron equation to PEO in PPO–PEO Langmuir films. *Adv. Colloid Interface Sci*. **222**, 199–214. (doi:10.1016/j.cis.2014.11.002)
56. Vollhardt D. 2014 Brewster angle microscopy: a preferential method for mesoscopic characterization of monolayers at the air/water interface. *Curr. Opin. Colloid Interface Sci*. **19**, 183–197. (doi:10.1016/j.cocis.2014.02.001)
57. Hoenig D, Moebius D. 1991 Direct visualization of monolayers at the air-water interface by Brewster angle microscopy. *J. Phys. Chem*. **95**, 4590–4592. (doi:10.1021/j100165a003)
58. Kawaguchi M, Tohyama M, Mutoh Y, Takahashi A. 1988 Ellipsometric study of polymer monolayers spread at the air water interface.1. Thickness of monolayers. *Langmuir* **4**, 407–410. (doi:10.1021/la00080a025)
59. Reiter R, Motschmann H, Orendi H, Nemetz A, Knoll W. 1992 Ellipsometric microscopy - imaging monomolecular surfactant layers at the air-water-interface. *Langmuir* **8**, 1784–1788. (doi:10.1021/la00043a017)
60. Kim YS, Snively CM, Liu YJ, Rabolt JF, Chase DB. 2008 Real-time imaging of crystallization in polylactide enantiomeric monolayers at the air-water interface. *Langmuir* **24**, 10 791–10 796. (doi:10.1021/la801747k)
61. Mendelsohn R, Mao G, Flach CR. 2010 Infrared reflection–absorption spectroscopy: principles and applications to lipid–protein interaction in Langmuir films. *Biochim. Biophys. Acta, Biomembr*. **1798**, 788–800. (doi:10.1016/j.bbamem.2009.11.024)
62. Bourque H, Laurin I, Pézolet M, Klass JM, Lennox RB, Brown GR. 2001 Investigation of the poly(l-lactide)/poly(d-lactide) stereocomplex at the air—water interface by polarization modulation infrared reflection absorption spectroscopy. *Langmuir* **17**, 5842–5849. (doi:10.1021/la0009792)
63. Weidemann G, Brezesinski G, Vollhardt D, Mohwald H. 1998 Texture change separate from the transition between two tilted phases in Langmuir monolayers. *J. Phys. Chem. B* **102**, 1224–1228. (doi:10.1021/jp972777t)
64. Broniatowski M, Flasiński M, Dynarowicz-Łątka P, Majewski J. 2010 Grazing incidence diffraction and X-ray reflectivity studies of the interactions of inorganic mercury salts with membrane lipids in Langmuir monolayers at the air/water interface. *J. Phys. Chem. B* **114**, 9474–9484. (doi:10.1021/jp101668n)
65. Zhavnerko G, Marletta G. 2010 Developing Langmuir-Blodgett strategies towards practical devices. *Mater. Sci. Eng. B* **169**, 43–48. (doi:10.1016/j.mseb.2009.12.005)
66. Ulman A. 1991 Part Two - Langmuir–Blodgett films. In *An introduction to ultrathin organic films* (ed. A Ulman), pp. 101–236. San Diego, CA: Academic Press.
67. Langmuir I, Schaefer VJ. 1938 Activities of urease and pepsin monolayers. *J. Am. Chem. Soc*. **60**, 1351–1360. (doi:10.1021/ja01273a023)
68. Pohjakallio M, Aho T, Kontturi K, Kontturi E. 2011 Morphology of poly(methyl methacrylate) and polystyrene blends upon Langmuir-Schaefer deposition. *Soft Matter* **7**, 743–748. (doi:10.1039/C0SM00360C)
69. Petty MC. 1996 *Langmuir-Blodgett* films: an introduction. Cambridge, UK: Cambridge University Press.
70. Roberts GG. 1990 *Langmuir-Blodgett films*. New York, NY: Springer US.
71. Kumaki J. 2016 Observation of polymer chain structures in two-dimensional films by atomic force microscopy. *Polym. J*. **48**, 3–14. (doi:10.1038/pj.2015.67)
72. Wang X, Wen G, Huang C, Wang Z, Shi Y. 2014 Aggregation behavior of the blends of PS-b-PEO-b-PS and PS-b-PMMA at the air/water interface. *RSC Adv*. **4**, 49 219–49 227. (doi:10.1039/C4RA08579E)
73. Claro PCD, Coustet ME, Diaz C, Maza E, Cortizo MS, Requejo FG, Pietrasanta LI, Ceolin M, Azzaroni O. 2013 Self-assembly of PBzMA-b-PDMAEMA diblock copolymer films at the air-water interface and deposition on solid substrates via Langmuir-Blodgett transfer. *Soft Matter* **9**, 10 899–10 912. (doi:10.1039/c3sm52336e)
74. Pandey RK, Upadhyay C, Prakash R. 2013 Pressure dependent surface morphology and Raman studies of semicrystalline poly(indole-5-carboxylic acid) by the Langmuir-Blodgett technique. *RSC Adv*. **3**, 15 712–15 718. (doi:10.1039/c3ra41895b)
75. Matharu Z, Sumana G, Gupta V, Malhotra BD. 2010 Langmuir–Blodgett films of polyaniline for low density lipoprotein detection. *Thin Solid Films* **519**, 1110–1114. (doi:10.1016/j.tsf.2010.08.053)
76. Boury F, Gulik A, Dedieu JC, Proust JE. 1994 First-order transition in a polymer monolayer: structural analysis by transmission electronic microscopy and atomic force microscopy. *Langmuir* **10**, 1654–1656. (doi:10.1021/la00018a006)
77. Price EW, Guo Y, Wang CW, Moffitt MG. 2009 Block copolymer strands with internal microphase separation structure via self-assembly at the air—water interface. *Langmuir* **25**, 6398–6406. (doi:10.1021/la804317s)
78. Geiß G, Hickel W, Lupo D, Praß W, Scheunemann U. 1991 Ellipsometry on anisotropic Langmuir-Blodgett films. *Ber. Bunsen-Ges*. **95**, 1345–1349. (doi:10.1002/bbpc.19910951106)
79. Haro M, Gascón I, Aroca R, López MC, Royo FM. 2008 Structural characterization and properties of an azopolymer arranged in Langmuir and Langmuir–Blodgett films. *J. Colloid Interface Sci*. **319**, 277–286. (doi:10.1016/j.jcis.2007.10.009)
80. Debnath P, Chakraborty S, Deb S, Nath J, Bhattacharjee D, Hussain SA. 2015 Reversible transition between excimer and J-aggregate of indocarbocyanine dye in Langmuir–Blodgett (LB) films. *J. Phys. Chem. C* **119**, 9429–9441. (doi:10.1021/acs.jpcc.5b02111)
81. Huie Z, Yu G, Shunsuke Y, Tokuji M, Masaya M. 2016 Angle-resolved X-ray photoelectron spectroscopy study of poly(vinylidene fluoride)/poly(N -dodecylacrylamide) Langmuir–Blodgett nanofilms. *Jpn. J. Appl. Phys*. **55**, 03DD11. (doi:10.7567/JJAP.55.03DD11)
82. Ulman A. 1990 Fourier Transform infrared spectroscopy of Langmuir—Blodgett and self-assembled films. In *ACS Symposium Series on Fourier transform infrared spectroscopy in colloid and interface science*, pp. 144–159. Washington, DC: American Chemical Society.
83. Tredgold RH. 1987 Langmuir-Blodgett films made from preformed polymers. *Thin Solid Films* **152**, 223–230. (doi:10.1016/0040-6090(87)90418-4)
84. Schmidt A, Mathauer K, Reiter G, Foster MD, Stamm M, Wegner G, Knoll W. 1994 Self-diffusion of hairy rod molecules in Langmuir-Blodgett-Kuhn multilayers probed with neutron and X-Ray reflectometry. *Langmuir* **10**, 3820–3826. (doi:10.1021/la00022a070)
85. Li B, Wu Y, Liu M, Esker AR. 2006 Brewster angle microscopy study of poly(ε-caprolactone) crystal growth in Langmuir films at the air/water interface. *Langmuir* **22**, 4902–4905. (doi:10.1021/la060048b)
86. Tredgold RH, Vickers AJ, Hoorfar A, Hodge P, Khoshdel E. 1985 X-ray analysis of some porphyrin and polymer Langmuir-Blodgett films. *J. Phys. D: Appl. Phys*. **18**, 1139–1145. (doi:10.1088/0022-3727/18/6/017)
87. Schulz B, Dietzel B, Kaminorz Y. 2001 Supramolecular structure and electro-optical properties of functionalized maleic anhydride copolymers. *Macromol. Symp*. **164**, 457–464. (doi:10.1002/1521-3900(200102)164:1<457::AID-MASY457>3.0.CO;2-E)

88. Bernardini C, Stuart MAC, Stoyanov SD, Arnaudov LN, Leermakers FAM. 2012 Polymer compatibility in two dimensions. Modeling of phase behavior of mixed polymethacrylate Langmuir films. *Langmuir* **28**, 5614–5621. (doi:10.1021/la2040642)
89. Glagola CP, Miceli LM, Milchak MA, Halle EH, Logan JL. 2012 Polystyrene–poly(ethylene oxide) diblock copolymer: the effect of polystyrene and spreading concentration at the air/water interface. *Langmuir* **28**, 5048–5058. (doi:10.1021/la204100d)
90. Deschênes L, Bousmina M, Ritcey AM. 2008 Micellization of PEO/PS block copolymers at the air/water interface: a simple model for predicting the size and aggregation number of circular surface micelles. *Langmuir* **24**, 3699–3708. (doi:10.1021/la702141h)
91. Kim HC, Lee H, Khetan J, Won Y-Y. 2015 Surface mechanical and rheological behaviors of biocompatible poly((d,l-lactic acid-ran-glycolic acid)-block-ethylene glycol) (PLGA–PEG) and poly((d,l-lactic acid-ran-glycolic acid-ran-ε-caprolactone)-block-ethylene glycol) (PLGACL–PEG) block copolymers at the air–water interface. *Langmuir* **31**, 13 821–13 833. (doi:10.1021/acs.langmuir.5b03622)
92. Schulze M, Seufert M, Fakirov C, Tebbe H, Buchholz V, Wegner G. 1997 Supramolecular architectures of cellulose derivatives. *Macromol. Symp*. **120**, 237–245. (doi:10.1002/masy.19971200124)
93. Tredgold RH. 1994 More complex structures formed by the Langmuir–Blodgett technique. In *Order in thin organic films* (ed. RH Tredgold). Cambridge, UK: Cambridge University Press.
94. Mabuchi M, Kobata S, Ito S, Yamamoto M, Schmidt A, Knoll W. 1998 Preparation and characterization of the Langmuir—Blodgett films made of hairy-rod polyglutamates bearing various chromophores in the side chain. *Langmuir* **14**, 7260–7266. (doi:10.1021/la980555w)
95. Schwiegk S, Vahlenkamp T, Xu Y, Wegner G. 1992 Origin of orientation phenomena observed in layered Langmuir-Blodgett structures of hairy-rod polymers. *Macromolecules* **25**, 2513–2525. (doi:10.1021/ma00035a034)
96. Fujimori A, Miura S, Kikkawa T, Shibasaki Y. 2015 Fine structural analysis, formation of interfacial particle films, and accurate estimation of orientation in polyguanamine derivatives with a high refractive index. *J. Polym. Sci. B Polym. Phys*. **53**, 999–1009. (doi:10.1002/polb.23728)
97. Woodruff MA, Hutmacher DW. 2010 The return of a forgotten polymer—Polycaprolactone in the 21st century. *Prog. Polym. Sci*. **35**, 1217. (doi:10.1016/j.progpolymsci.2010.04.002)
98. Sisson AL, Ekinci D, Lendlein A. 2013 The contemporary role of ε-caprolactone chemistry to create advanced polymer architectures. *Polymer* **54**, 4333–4350. (doi:10.1016/j.polymer.2013.04.045)
99. Huang MH, Li SM, Hutmacher DW, Schantz JT, Vacanti CA, Braud C, Vert M. 2004 Degradation and cell culture studies on block copolymers prepared by ring opening polymerization of epsilon-caprolactone in the presence of poly(ethylene glycol). *J. Biomed. Mater. Res. A* **69a**, 417–427. (doi:10.1002/jbm.a.30008)
100. Leiva A, Gargallo L, Radić D. 2004 Interfacial properties of poly(caprolactone) and derivatives. *J. Macromol. Sci. A Pure Appl. Chem*. **41**, 577–583. (doi:10.1081/MA-120030926)
101. Li B. 2004 Surface Characterization Of Poly(ε-caprolactone) at the air/water interface. Master thesis, Virginia, Virginia Polytechnic Institute and State University, Blacksburg.
102. Li BB, Esker AR. 2007 Molar mass dependent growth of poly(epsilon-caprolactone) crystals in Langmuir films. *Langmuir* **23**, 2546–2554. (doi:10.1021/la062563f)
103. Li B, Esker AR. 2006 Blends of poly(ε-caprolactone) and intermediate molar mass polystyrene as Langmuir films at the air/water interface. *Langmuir* **23**, 574–581. (doi:10.1021/la0625291)
104. Hottle JR, Deng J, Kim H-J, Farmer-Creely CE, Viers BD, Esker AR. 2005 Blends of amphiphilic poly(dimethylsiloxane) and nonamphiphilic octaisobutyl-POSS at the air/water interface. *Langmuir* **21**, 2250–2259. (doi:10.1021/la047565j)
105. Schöne A-C, Kratz K, Schulz B, Reiche J, Santer S, Lendlein A. 2015 Surface pressure-induced isothermal 2D- to 3D-transitions in Langmuir films of poly(ε-caprolactone)s and oligo(ε-caprolactone) based polyesterurethanes. *Polym. Adv. Technol*. **26**, 1411–1420. (doi:10.1002/pat.3638)
106. Joncheray TJ, Denoncourt KM, Mathieu C, Meier MAR, Schubert US, Duran RS. 2006 Langmuir and Langmuir—Blodgett Films of Poly(ethylene oxide)-b-Poly(ε-caprolactone) star-shaped block copolymers. *Langmuir* **22**, 9264–9271. (doi:10.1021/la061290l)
107. Naolou T, Busse K, Lechner B-D, Kressler J. 2014 The behavior of poly(ε-caprolactone) and poly(ethylene oxide)-b-poly(ε-caprolactone) grafted to a poly(glycerol adipate) backbone at the air/water interface. *Colloid Polym. Sci*. **292**, 1199–1208. (doi:10.1007/s00396-014-3168-1)
108. Reiche J, Kulkarni A, Kratz K, Lendlein A. 2008 Enzymatic monolayer degradation study of multiblock copolymers consisting of poly(ε-caprolactone) and poly(p-dioxanone) blocks. *Thin Solid Films* **516**, 8821–8828. (doi:10.1016/j.tsf.2007.11.053)
109. Ringard-Lefebvre C, Baszkin A. 1994 Main transition-like feature in polylactic acid Langmuir films. *Langmuir* **10**, 2376–2381. (doi:10.1021/la00019a057)
110. Klass JM, Lennox RB, Brown GR, Bourque H, Pézolet M. 2003 Enantiomeric polylactides at the air—water interface: π—A isotherms and PM-IRRAS studies of enantiomers and their blend. *Langmuir* **19**, 333–340. (doi:10.1021/la020606w)
111. Boury F, Olivier E, Proust JE, Benoit JP. 1993 A study of poly(α-hydroxy acid)s monolayers spread at the air/water interface: influence of the d,l-lactic acid/glycolic acid ratio. *J. Colloid Interface Sci*. **160**, 1–9. (doi:10.1006/jcis.1993.1361)
112. Park HW, Choi J, Ohn K, Lee H, Kim JW, Won YY. 2012 Study of the air-water interfacial properties of biodegradable polyesters and their block copolymers with poly(ethylene glycol). *Langmuir* **28**, 11 555–11 566. (doi:10.1021/La300810q)
113. Boury F, Saulnier P, Proust JE, Panaïotov I, Ivanova T, Postel C, Abillon O. 1999 Characterization of the morphology of poly(α-hydroxy acid)s Langmuir–Blodgett films by atomic force microscopy measurements. *Colloids Surf. A* **155**, 117–129. (doi:10.1016/S0927-7757(98)00705-5)
114. Schöne AC, Richau K, Kratz K, Schulz B, Lendlein A. 2015 Influence of diurethane linkers on the Langmuir layer behavior of oligo[(rac-lactide)-co-glycolide]-based polyesterurethanes. *Macromol. Rapid Commun*. **36**, 1910–1915. (doi:10.1002/marc.201500316)
115. Kim HC, Lee H, Jung H, Choi YH, Meron M, Lin B, Bang J, Won Y-Y. 2015 Humidity-dependent compression-induced glass transition of the air-water interfacial Langmuir films of poly(d,l-lactic acid-ran-glycolic acid) (PLGA). *Soft Matter* **11**, 5666–5677. (doi:10.1039/C4SM02535K)
116. Wang K, Zhou C, Hong Y, Zhang X. 2012 A review of protein adsorption on bioceramics. *Interface Focus* **2**, 259–277. (doi:10.1098/rsfs.2012.0012)
117. Camarero JA. 2008 Recent developments in the site-specific immobilization of proteins onto solid supports. *Pept. Sci*. **90**, 450–458. (doi:10.1002/bip.20803)
118. Cumper CWN, Alexander AE. 1950 The surface chemistry of proteins. *Trans. Faraday Soc*. **46**, 235–253. (doi:10.1039/tf9504600235)
119. Furuno T. 2014 Atomic force microscopy study on the unfolding of globular proteins in the Langmuir films. *Thin Solid Films* **552**, 170–179. (doi:10.1016/j.tsf.2013.12.052)
120. Gani SA, Mukherjee DC, Chattoraj DK. 1999 Adsorption of biopolymer at solid-liquid interfaces. 2. Interaction of BSA and DNA with casein. *Langmuir* **15**, 7139–7144. (doi:10.1021/la970687+)
121. Sanchez-Gonzalez J, Ruiz-Garcia J, Galvez-Ruiz MJ. 2003 Langmuir-Blodgett films of biopolymers: a method to obtain protein multilayers. *J. Colloid Interface Sci*. **267**, 286–293. (doi:10.1016/S0021-9797(03)00754-9)
122. Reviakine I, Jung F, Braune S, Brash JL, Latour R, Gorbet M, van Oeveren W. 2017 Stirred, shaken, or stagnant: What goes on at the blood–biomaterial interface. *Blood Rev*. **31**, 11–21. (doi:10.1016/j.blre.2016.07.003)
123. Miao S, Leeman H, De Feyter S, Schoonheydt RA. 2010 Facile preparation of Langmuir-Blodgett films of water-soluble proteins and hybrid protein-clay films. *J. Mater. Chem*. **20**, 698–705. (doi:10.1039/b913659b)
124. McClellan SJ, Franses EI. 2003 Effect of concentration and denaturation on adsorption and surface tension of bovine serum albumin. *Colloids Surf. B* **28**, 63–75. (doi:10.1016/S0927-7765(02)00131-5)
125. Pedraz P, Montes FJ, Cerro RL, Diaz ME. 2012 Characterization of Langmuir biofilms built by the biospecific interaction of arachidic acid with bovine

serum albumin. *Thin Solid Films* **525**, 121–131. (doi:10.1016/j.tsf.2012.10.055)

126. Noskov BA, Mikhailovskaya AA, Lin SY, Loglio G, Miller R. 2010 Bovine serum albumin unfolding at the air/water interface as studied by dilational surface rheology. *Langmuir* **26**, 17 225–17 231. (doi:10.1021/la103360h)
127. Sanchez-Gonzalez J, Cabrerizo-Vilchez MA, Galvez-Ruiz MJ. 2001 Interactions, desorption and mixing thermodynamics in mixed monolayers of beta-lactoglobulin and bovine serum albumin. *Colloids Surf. B* **21**, 19–27. (doi:10.1016/S0927-7765(01)00180-1)
128. Engelhardt K, Rumpel A, Walter J, Dombrowski J, Kulozik U, Braunschweig B, Peukert W. 2012 Protein adsorption at the electrified air-water interface: implications on foam stability. *Langmuir* **28**, 7780–7787. (doi:10.1021/la301368v)
129. Engelhardt K, Peukert W, Braunschweig B. 2014 Vibrational sum-frequency generation at protein modified air-water interfaces: effects of molecular structure and surface charging. *Curr. Opin. Colloid Interface Sci.* **19**, 207–215. (doi:10.1016/j.cocis.2014.03.008)
130. Lu JR, Su TJ, Penfold J. 1999 Adsorption of serum albumins at the air/water interface. *Langmuir* **15**, 6975–6983. (doi:10.1021/la990131h)
131. Toimil P, Prieto G, Miñones Jr J, Trillo JM, Sarmiento F. 2012 Monolayer and Brewster angle microscopy study of human serum albumin—Dipalmitoyl phosphatidyl choline mixtures at the air–water interface. *Colloids Surf. B* **92**, 64–73. (doi:10.1016/j.colsurfb.2011.11.022)
132. Lu JR, Su TJ, Thomas RK. 1999 Structural conformation of bovine serum albumin layers at the air-water interface studied by neutron reflection. *J. Colloid Interface Sci.* **213**, 426–437. (doi:10.1006/jcis.1999.6157)
133. Campbell RA, Ang JC, Sebastiani F, Tummino A, White JW. 2015 Spread films of human serum albumin at the air-water interface: optimization, morphology, and durability. *Langmuir* **31**, 13 535–13 542. (doi:10.1021/acs.langmuir.5b03349)
134. Damodaran S. 2003 In situ measurement of conformational changes in proteins at liquid interfaces by circular dichroism spectroscopy. *Anal. Bioanal. Chem.* **376**, 182–188. (doi:10.1007/s00216-003-1873-6)
135. Sessions K, Sacks S, Li SH, Leblanc RM. 2014 epi-Fluorescence imaging at the air-water interface of fibrillization of bovine serum albumin and human insulin. *Chem. Commun.* **50**, 8955–8957. (doi:10.1039/c4cc04030a)
136. Owaku K, Shinohara H, Ikariyama Y, Aizawa M. 1989 Preparation and characterization of protein Langmuir-Blodgett films. *Thin Solid Films* **180**, 61–64. (doi:10.1016/0040-6090(89)90054-0)
137. Latnikova AV, Lin SY, Loglio G, Miller R, Noskov BA. 2008 Impact of surfactant additions on dynamic properties of beta-casein adsorption layers. *J. Phys. Chem. C* **112**, 6126–6131. (doi:10.1021/jp712107n)
138. Holly FJ, Dolowy K, Yamada KM. 1984 comparative surface chemical studies of cellular fibronectin and submaxillary mucin monolayers - effects of ph, ionic-strength, and presence of calcium-ions. *J. Colloid Interface Sci.* **100**, 210–215. (doi:10.1016/0021-9797(84)90427-2)
139. Bhuvanesh T *et al.* In press. Langmuir–Schaefer films of fibronectin as designed biointerfaces for culturing stem cells. *Polym. Adv. Technol.* (doi:10.1002/pat.3910)
140. Thakur G, Wang CS, Leblanc RA. 2008 Surface chemistry and in situ spectroscopy of a lysozyme Langmuir monolayer. *Langmuir* **24**, 4888–4893. (doi:10.1021/la703893m)
141. Yano YF, Kobayashi Y, Ina T, Nitta K, Uruga T. 2016 Hofmeister anion effects on protein adsorption at an air-water interface. *Langmuir* **32**, 9892–9898. (doi:10.1021/acs.langmuir.6b02352)
142. Lad MD, Birembaut F, Matthew JM, Frazier RA, Green RJ. 2006 The adsorbed conformation of globular proteins at the air/water interface. *Phys. Chem. Chem. Phys.* **8**, 2179–2186. (doi:10.1039/b515934b)
143. Bos MA, van Vliet T. 2001 Interfacial rheological properties of adsorbed protein layers and surfactants: a review. *Adv. Colloid Interface Sci.* **91**, 437–471. (doi:10.1016/S0001-8686(00)00077-4)
144. Cicuta P. 2007 Compression and shear surface rheology in spread layers of beta-casein and beta-lactoglobulin. *J. Colloid Interface Sci.* **308**, 93–99. (doi:10.1016/j.jcis.2006.12.056)
145. Sengupta T, Razumovsky L, Damodaran S. 1999 Energetics of protein—interface interactions and its effect on protein adsorption. *Langmuir* **15**, 6991–7001. (doi:10.1021/la990235s)
146. Perriman AW, Henderson MJ, Holt SA, White JW. 2007 Effect of the air-water interface on the stability of beta-lactoglobulin. *J. Phys. Chem. B* **111**, 13 527–13 537. (doi:10.1021/jp074777r)
147. Ambroggio EE, Caruso B, Villarreal MA, Raussens V, Fidelio GD. 2016 Reversing the peptide sequence impacts on molecular surface behaviour. *Colloids Surf. B* **139**, 25–32. (doi:10.1016/j.colsurfb.2015.12.008)
148. Ambroggio EE, Fidelio GD. 2013 Lipid-like behavior of signal sequence peptides at air–water interface. *Biochim. Biophys. Acta, Biomembr.* **1828**, 708–714. (doi:10.1016/j.bbamem.2012.11.004)
149. Yokoi H, Hayashi S, Kinoshita T. 2003 Polypeptide membranes at an interface. *Prog. Polym. Sci.* **28**, 341–357. (doi:10.1016/S0079-6700(02)00081-3)
150. Reiter R, Wintzenrieth F, Reiter G. 2016 Self-assembly behavior of a rod-like polypeptide at the air-water interface. *Polymer* **107**, 379–386. (doi:10.1016/j.polymer.2016.08.023)
151. Shin S, Ahn S, Cheng J, Chang H, Jung D-H, Hyun J. 2016 Morphological variation of stimuli-responsive polypeptide at air–water interface. *Appl. Surf. Sci.* **388**, 551–556. (doi:10.1016/j.apsusc.2015.10.126)
152. Kato N, Sasaki T, Mukai Y. 2015 Partially induced transition from horizontal to vertical orientation of helical peptides at the air–water interface and the structure of their monolayers transferred on the solid substrates. *Biochim. Biophys. Acta, Biomembr.* **1848**, 967–975. (doi:10.1016/j.bbamem.2014.12.022)
153. Li S, Leblanc RM. 2014 Aggregation of insulin at the interface. *J. Phys. Chem. B* **118**, 1181–1188. (doi:10.1021/jp4101202)
154. Johnson S, Liu W, Thakur G, Dadlani A, Patel R, Orbulescu J, Whyte JD, Micic M, Leblanc RM. 2012 Surface chemistry and spectroscopy of human insulin Langmuir monolayer. *J. Phys. Chem. B* **116**, 10 205–10 212. (doi:10.1021/jp3046643)
155. Liu W, Johnson S, Micic M, Orbulescu J, Whyte J, Garcia AR, Leblanc RM. 2012 Study of the aggregation of human insulin Langmuir monolayer. *Langmuir* **28**, 3369–3377. (doi:10.1021/la204201w)
156. Nieto-Suarez M, Vila-Romeu N, Prieto I. 2008 Behaviour of insulin Langmuir monolayers at the air-water interface under various conditions. *Thin Solid Films* **516**, 8873–8879. (doi:10.1016/j.tsf.2007.11.062)
157. Kubies D, Machova L, Brynda E, Lukas J, Rypacek F. 2003 Functionalized surfaces of polylactide modified by Langmuir-Blodgett films of amphiphilic block copolymers. *J. Mater. Sci.: Mater. Med.* **14**, 143–149. (doi:10.1023/A:1022019813078)
158. Vert M. 2015 After soft tissues, bone, drug delivery and packaging, PLA aims at blood. *Eur. Polym. J.* **68**, 516–525. (doi:10.1016/j.eurpolymj.2015.03.051)
159. Ishaug SL, Yaszemski MJ, Bizios R, Mikos AG. 1994 Osteoblast function on synthetic biodegradable polymers. *J. Biomed. Mater. Res.* **28**, 1445–1453. (doi:10.1002/jbm.820281210)
160. Kiss É, Dravetzky K, Hill K, Kutnyánszky E, Varga A. 2008 Protein interaction with a pluronic-modified poly(lactic acid) Langmuir monolayer. *J. Colloid Interface Sci.* **325**, 337–345. (doi:10.1016/j.jcis.2008.05.057)
161. Hlady V, Jogikalmath G. 2007 Albumin binding and insertion into PS-b-PEO monolayers at air–water interface. *Colloids Surf., B* **54**, 179–187. (doi:10.1016/j.colsurfb.2006.10.018)
162. Boury F, Ivanova T, Panaieotov I, Proust JE. 1995 Dilatational properties of poly(dl-lactic acid) and bovine serum albumin monolayers spread at the air/water interface. *Langmuir* **11**, 599–606. (doi:10.1021/la00002a040)
163. Schöne AC, Falkenhagen S, Travkova O, Schulz B, Kratz K, Lendlein A. 2015 Influence of intermediate degradation products on the hydrolytic degradation of poly [(rac-lactide)-co-glycolide] at the air-water interface. *Polym. Adv. Technol.* **26**, 1402–1410. (doi:10.1002/pat.3701)
164. Lee WK, Nowak RW, Gardella JA. 2002 Hydrolytic degradation of polyester blend monolayers at the air/water interface: effects of a slowly degrading component. *Langmuir* **18**, 2309–2312. (doi:10.1021/La011663c)
165. Kulkarni A, Reiche J, Lendlein A. 2007 Hydrolytic degradation of poly(rac-lactide) and poly[(rac-lactide)-co-glycolide] at the air-water interface. *Surf. Interface Anal.* **39**, 740–746. (doi:10.1002/Sia.2580)
166. Kulkarni A, Reiche J, Kratz K, Kamusewitz H, Sokolov IM, Lendlein A. 2007 Enzymatic chain scission

kinetics of Poly(epsilon-caprolactone) monolayers. *Langmuir* **23**, 12 202–12 207. (doi:10.1021/La701523e)

167. Wang M, Smith JM, McCoy BJ. 1995 Continuous kinetics for thermal degradation of polymer in solution. *AlChE J.* **41**, 1521–1533. (doi:10.1002/aic.690410616)
168. Reiche J, Kratz K, Hofmann D, Lendlein A. 2011 Current status of Langmuir monolayer degradation of polymeric biomaterials. *Int. J. Artif. Organs* **34**, 123–128. (doi:10.5301/ijao.2011.6401)
169. Ivanova T, Panaiotov I, Boury F, Proust JE, Benoit JP, Verger R. 1997 Hydrolysis kinetics of poly(D,L-lactide) monolayers spread on basic or acidic aqueous subphases. *Colloids Surf. B* **8**, 217–225. (doi:10.1016/S0927-7765(96)01331-8)
170. van Nostrum CF, Veldhuis TFJ, Bos GW, Hennink WE. 2004 Hydrolytic degradation of oligo(lactic acid): a kinetic and mechanistic study. *Polymer* **45**, 6779–6787. (doi:10.1016/j.polymer.2004.08.001)
171. Lee JK, Ryon JH, Lee WK, Park CY, Park SB, Min SK. 2003 Study on hydrolytic kinetics of Langmuir monolayers of biodegradable polylactide derivatives. *Macromol. Res*. **11**, 476–480. (doi:10.1007/BF03218979)
172. Shakesheff KM. 2011 Drug delivery systems. In *Handbook of biodegradable polymers* (eds A Lendlein, AL Sisson), pp. 363–378. Weinheim, Germany: Wiley-VCH Verlag GmbH & Co. KGaA.
173. Lee WK, Iwata T, Gardella JA. 2005 Hydrolytic behavior of enantiomeric poly(lactide) mixed monolayer films at the air/water interface: stereocomplexation effects. *Langmuir* **21**, 11 180–11 184. (doi:10.1021/La051137b)
174. Andersson SR, Hakkarainen M, Inkinen S, Södergård A, Albertsson A-C. 2010 Polylactide stereocomplexation leads to higher hydrolytic stability but more acidic hydrolysis product pattern. *Biomacromolecules* **11**, 1067–1073. (doi:10.1021/bm100029t)
175. Lee WK, Gardella JA. 2000 Hydrolytic kinetics of biodegradable polyester monolayers. *Langmuir* **16**, 3401–3406. (doi:10.1021/La990800r)
176. Ivanova T, Malzert A, Boury F, Proust JE, Verger R, Panaiotov I. 2003 Enzymatic hydrolysis by cutinase of PEG-co PLA copolymers spread monolayers. *Colloids Surf. B* **32**, 307–320. (doi:10.1016/j.colsurfb.2003.08.005)
177. Göpferich A. 1997 Polymer bulk erosion. *Macromolecules* **30**, 2598–2604. (doi:10.1021/ma961627y)
178. Grozev N, Svendsen A, Verger R, Panaiotov I. 2002 Enzymatic hydrolysis by Humicola lanuginosa lipase of polycaprolactone monolayers. *Colloid Polym. Sci.* **280**, 7–17. (doi:10.1007/s003960200001)
179. Li SM, Garreau H, Vert M. 1990 Structure property relationships in the case of the degradation of massive aliphatic poly-(alpha-hydroxy acids) in aqueous-media.1. Poly(dl-lactic acid). *J. Mater. Sci: Mater. Med.* **1**, 123–130. (doi:10.1007/Bf00700871)
180. Jo NJ, Iwata T, Lim KT, Jung SH, Lee WK. 2007 Degradation behaviors of polyester monolayers at the air/water interface: alkaline and enzymatic degradations. *Polym. Degrad. Stab*. **92**, 1199–1203. (doi:10.1016/j.polymdegradstab.2007.04.002)
181. Lambeek G, Vorenkamp EJ, Schouten AJ. 1995 Structural study of Langmuir-Blodgett monolayers and multilayers of poly(beta-hydroxybutyrate). *Macromolecules* **28**, 2023–2032. (doi:10.1021/ma00110a041)
182. Lendlein A. 1999 Polymere als Implantatwerkstoffe. *Chem. Unserer Zeit* **33**, 279–295. (doi:10.1002/ciuz.19990330505)
183. Peng H, Ling J, Liu J, Zhu N, Ni X, Shen Z. 2010 Controlled enzymatic degradation of poly(ε-caprolactone)-based copolymers in the presence of porcine pancreatic lipase. *Polym. Degrad. Stab*. **95**, 643–650. (doi:10.1016/j.polymdegradstab.2009.12.005)
184. Vidaurre A, Dueñas JMM, Estellés JM, Cortázar IC. 2008 Influence of enzymatic degradation on physical properties of poly(ε-caprolactone) films and sponges. *Macromol. Symp*. **269**, 38–46. (doi:10.1002/masy.200850907)
185. Miao ZM, Cheng SX, Zhang XZ, Wang QR, Zhuo RX. 2007 Degradation and drug release property of star poly(epsilon-caprolactone)s with dendritic cores. *J. Biomed. Mater. Res. B* **81b**, 40–49. (doi:10.1002/jbm.b.30634)
186. Kulkarni A, Reiche J, Hartmann J, Kratz K, Lendlein A. 2008 Selective enzymatic degradation of poly(epsilon-caprolactone) containing multiblock copolymers. *Eur. J. Pharm. Biopharm*. **68**, 46–56. (doi:10.1016/j.ejpb.2007.05.021)
187. Schöne A-C, Kratz K, Schulz B, Lendlein A. 2016 The relevance of hydrophobic segments in multiblock copolyesterurethanes for their enzymatic degradation at the air-water interface. *Polymer* **102**, 92–98. (doi:10.1016/j.polymer.2016.09.001)
188. Roßberg J, Rottke FO, Schulz B, Lendlein A. 2016 Enzymatic degradation of oligo(ε-caprolactone)s end-capped with phenylboronic acid derivatives at the air–water interface. *Macromol. Rapid Commun*. **37**, 1966–1971. (doi:10.1002/marc.201600471)
189. Schöne A-C, Kratz K, Schulz B, Lendlein A. 2016 Polymer architecture versus chemical structure as adjusting tools for the enzymatic degradation of oligo(ε-caprolactone) based films at the air-water interface. *Polym. Degrad. Stab*. **131**, 114–121. (doi:10.1016/j.polymdegradstab.2016.07.010)
190. Miller R, Ferri JK, Javadi A, Krägel J, Mucic N, Wüstneck R. 2010 Rheology of interfacial layers. *Colloid Polym. Sci*. **288**, 937–950. (doi:10.1007/s00396-010-2227-5)
191. Li Z, Ma X, Zang D, Guan X, Zhu L, Liu J, Chen F. 2015 Interfacial rheology and aggregation behaviour of amphiphilic CBABC-type pentablock copolymers at the air-water interface: effects of block ratio and chain length. *RSC Adv*. **5**, 82 869–82 878. (doi:10.1039/C5RA08109B)
192. Noskov BA, Loglio G, Miller R. 2011 Dilational surface visco-elasticity of polyelectrolyte/surfactant solutions: formation of heterogeneous adsorption layers. *Adv. Colloid Interface Sci*. **168**, 179–197. (doi:10.1016/j.cis.2011.02.010)
193. Kotsmar C *et al.* 2009 Thermodynamics, adsorption kinetics and rheology of mixed protein–surfactant interfacial layers. *Adv. Colloid Interface Sci*. **150**, 41–54. (doi:10.1016/j.cis.2009.05.002)
194. Maheshkumar J, Dhathathreyan A. 2013 Langmuir and Langmuir–Blodgett films of capsules of haemoglobin at air/water and solid/air interfaces. *J. Chem. Sci*. **125**, 219–227. (doi:10.1007/s12039-013-0370-5)
195. Grasso EJ, Oliveira RG, Maggio B. 2014 Rheological properties of regular insulin and aspart insulin Langmuir monolayers at the air/water interface: Condensing effect of $Zn^{2+}$ in the subphase. *Colloids Surf. B* **115**, 219–228. (doi:10.1016/j.colsurfb.2013.11.031)
196. Theodoratou A *et al.* 2016 Semifluorinated alkanes at the air–water interface: tailoring structure and rheology at the molecular scale. *Langmuir* **32**, 3139–3151. (doi:10.1021/acs.langmuir.5b04744)
197. Hofmann D, Entrialgo-Castaño M, Kratz K, Lendlein A. 2009 Knowledge-based approach towards hydrolytic degradation of polymer-based biomaterials. *Adv. Mater*. **21**, 3237–3245. (doi:10.1002/adma.200802213)